

Article

Enrichment of ATP binding proteins unveils proteomic alterations in human macrophage cell death, inflammatory response and protein synthesis after interaction with *Candida albicans*

Catarina Vaz, Jose Antonio Reales-Calderón, Aida Pitarch, María Luisa Hernáez, Perceval Vellosillo, Marco Trevisan-Herraz, Lucia Monteoliva, and Concha Gil

J. Proteome Res., **Just Accepted Manuscript** • DOI: 10.1021/acs.jproteome.9b00032 • Publication Date (Web): 15 Apr 2019

Downloaded from <http://pubs.acs.org> on April 22, 2019

Just Accepted

"Just Accepted" manuscripts have been peer-reviewed and accepted for publication. They are posted online prior to technical editing, formatting for publication and author proofing. The American Chemical Society provides "Just Accepted" as a service to the research community to expedite the dissemination of scientific material as soon as possible after acceptance. "Just Accepted" manuscripts appear in full in PDF format accompanied by an HTML abstract. "Just Accepted" manuscripts have been fully peer reviewed, but should not be considered the official version of record. They are citable by the Digital Object Identifier (DOI®). "Just Accepted" is an optional service offered to authors. Therefore, the "Just Accepted" Web site may not include all articles that will be published in the journal. After a manuscript is technically edited and formatted, it will be removed from the "Just Accepted" Web site and published as an ASAP article. Note that technical editing may introduce minor changes to the manuscript text and/or graphics which could affect content, and all legal disclaimers and ethical guidelines that apply to the journal pertain. ACS cannot be held responsible for errors or consequences arising from the use of information contained in these "Just Accepted" manuscripts.

1
2
3
4
5
6
7
8
9
10
11
12
13
14
15
16
17
18
19
20
21
22
23
24
25
26
27
28
29
30
31
32
33
34
35
36
37
38
39
40
41
42
43
44
45
46
47
48
49
50
51
52
53
54
55
56
57
58
59
60

Enrichment of ATP binding proteins unveils proteomic alterations in human macrophage cell death, inflammatory response and protein synthesis after interaction with *Candida* *albicans*

Catarina Vaz^{§&}, Jose Antonio Reales-Calderon^{§&†}, Aida Pitarch^{§&}, Perceval
Vellosillo[§], Marco Trevisan[▲], María Luisa Hernández[‡], Lucía Monteoliva^{§&*} and Concha
Gil^{§&‡}

AFFILIATION

[§] Departamento de Microbiología y Parasitología, Facultad de Farmacia, Universidad
Complutense de Madrid, Madrid, Spain

[&] Instituto Ramón y Cajal de Investigación Sanitaria IRYCIS, Madrid, Spain

[‡] Unidad de Proteómica, Universidad Complutense de Madrid, Madrid, Spain

[▲] Laboratorio de Proteómica Cardiovascular, Centro Nacional de Investigaciones
Cardiovasculares Carlos III (CNIC), Madrid, Spain

Corresponding author e-mail: luciamon@ucm.es

ABSTRACT

Macrophages are involved in the primary human response to *Candida albicans*. After pathogen recognition signaling pathways are activated, leading to the production of cytokines, chemokines and antimicrobial peptides. ATP binding proteins are crucial for this regulation. Here, a quantitative proteomic and phosphoproteomic approach was carried out for the study of human macrophage ATP-binding proteins after interaction with *C. albicans*. From a total of 547 non-redundant quantified proteins, 137 were ATP binding proteins and 59 were detected as differentially abundant. From the differentially abundant ATP-binding proteins, 6 were kinases (MAP2K2, SYK, STK3, MAP3K2, NDKA and SRPK1) most of them involved in signaling pathways. Furthermore, 85 phosphopeptides were quantified. Macrophage proteomic alterations including an increase of protein synthesis with a consistent decrease in proteolysis were observed. Besides, macrophages showed changes in proteins of endosomal trafficking together with mitochondrial proteins, including some involved in the response to oxidative stress. Regarding cell death mechanisms an increase of anti-apoptotic over pro-apoptotic signals was suggested. Furthermore, a high pro-inflammatory response was detected, together with no upregulation of key mi-RNAs involved in the negative feedback of this response. These findings illustrate a strategy to deepen the knowledge in the complex interactions between the host and the clinically important pathogen *C. albicans*.

Keywords: macrophages, *Candida albicans*, proteomics, SILAC, ATP binding proteins

INTRODUCTION

Candida albicans is a human opportunistic pathogen and a common commensal fungus of the mucosa from many healthy patients. Most potentially lethal invasive infections occur in immunocompromised patients, such as those infected with HIV or individuals with neutropenia owing to immunosuppressive treatments for cancer or organ transplantation.¹ Infections caused by *Candida* spp have high levels of morbidity and mortality particularly in critically ill patients that may be attributed to the difficulty in the early diagnosis of *Candida* infections and an appropriate antifungal therapy.² A recent epidemiologic study in Spain described a 30% of global mortality in the 705 documented cases of invasive candidiasis, and *C. albicans* was the most frequently isolated species, although an increase in non-*C. albicans* species has been observed.^{3,2} Macrophages, which are derived from monocytes circulating in the blood, are constantly patrolling tissues and non-sterile interfaces at the surfaces of epithelia, and are one of the key cells in the immune recognition and innate immune response to *C. albicans*.¹ These cells recognize and phagocyte *C. albicans*, eliciting innate immune responses through engagement of different pattern recognition receptors (PRRs) in an infection-stage specific manner.⁴ Mainly, PRRs are composed of three groups: Toll-like receptors (TLRs), C-type lectin receptors (CLRs) and nod-like receptors (NODs). These PRRs, which include multiple cell-bound receptors (such as TLR2 and 4, Dectin-1 or Mannan Receptor), soluble receptors (like galectin-3), and intracellular receptors (like TLR 9), activate several signal transduction pathways, which finally lead to the upregulation of costimulatory molecules and the production of inflammatory cytokines, chemokines, antimicrobial peptides, and type I interferons (IFNs).⁵ Our research group identified new differentially abundant proteins in *C. albicans*-stimulated RAW 264.7 macrophages using proteomic approaches.⁶⁻⁷

Differentially abundant proteins were suggested to have pro-inflammatory and anti-apoptotic effects.⁶⁻⁷ Another study on human M1 (classically activated, pro-inflammatory subtype) and M2 (alternatively activated, anti-inflammatory subtype) macrophages showed that the biggest differences between them were related to cytoskeletal rearrangement and metabolic routes⁸. Other studies analyzed the interaction between macrophage and *Candida* using proteomic approaches, and found proteins involved in energy metabolism, cell survival and candidates for interaction-specific molecules.⁹⁻¹⁰

Adenosine triphosphate (ATP) can bind to a group of proteins known as ATP-binding proteins. ATP-binding proteins were previously studied to elucidate molecular mechanisms in cancer, identify proteins that can be therapeutic targets for the development of novel antibiotics, and profile plant proteomes.¹¹⁻¹⁴ However, their role is still poorly understood during different infection scenarios. This group of proteins include kinases, heat shock proteins as well as ATPases, and are crucial in several cellular processes, such as cell signaling, protein synthesis and metabolism.¹⁵ Despite the importance of these proteins in those pivotal cellular functions, proteomic studies of ATP-binding proteins by MS are still a challenge mainly due to the fact that some ATP-binding proteins are present at very low cellular concentrations.¹⁶ The combination of MS instrumentation with powerful separation techniques or selective enrichment of these proteins and bioinformatics tools can help in the identification and quantification of low abundant proteins in complex samples.¹¹ Several procedures for selective enrichment of ATP binding proteins and kinases have been developed^{11, 17-20}, including a probe-based technology that uses biotinylated acyl phosphates of ATP or adenosine diphosphate (ADP) that irreversibly react with protein kinases on conserved lysine residues in the ATP binding pocket.²¹ These probes covalently label the active site of

ATPases, including chaperones and metabolic enzymes, to enable their selective enrichment using a desthiobiotin tag. The combination of metabolic labelling, such as stable isotope labeling by amino acids in cell culture (SILAC), with affinity enrichment was proven previously to be useful for quantification of subproteomes of interest.²²⁻²³ Moreover, protein post-translational modifications (PTMs) play a crucial role in the regulation of several biological processes, such as cell signalling, immune response, recognition of pathogens, among others. More than 300 types of protein PTMs are known to occur physiologically within living organisms. From these PTMs, the phosphorylation is highly important during signal transduction and it is believed that more than 30% of the proteins can be phosphorylated.²⁴ A better understanding of the immune response during fungal infection may help in the development of new improved therapies in the future. We are particularly interested in unravelling new regulatory mechanisms activated by macrophages after interaction with *C. albicans*. Here, we study the abundances and phosphorylation levels of ATP-binding proteins in human macrophage cells after interacting with *C. albicans*. For that, SILAC was used to differentially label proteomes obtained from control macrophages and macrophages after interaction with *C. albicans*. The combined cell lysates were subjected to ATP-binding protein enrichment and a quantitative proteomic and phosphoproteomic approach was used to analyze the enriched extracts.

MATERIALS AND METHODS

C. albicans strain

The *C. albicans* SC5314 strain was used in this study. This strain was grown in YPD plates (2% glucose, 1% yeast extract, 2% peptone and 2% agar) at 30°C.

THP-1 cell culture and macrophage differentiation

The human acute monocytic leukemia cell line (THP-1) was cultured in Dulbecco's modified eagle's (DMEM) medium supplemented with antibiotics (penicillin 10000 U/ml-streptomycin 10000U/ml), 2 mM L-glutamine and 10% heat-inactivated fetal bovine serum (FBS) at 37°C in a humidified atmosphere containing 5% CO₂. THP-1 cells were seeded in 24-well plastic plates at a density of 1x10⁶ cells/well in complete medium and treated with a final concentration of 30 ng/ml phorbol 12-myristate 13-acetate (PMA; Sigma-Aldrich) for 48 h to induce maturation toward adherent macrophage-like cells. After 48 h cultures, the medium containing PMA was replaced with fresh medium without PMA to remove unattached cells.

C. albicans-macrophage co-culture

For interaction studies, THP-1 macrophages were incubated with *C. albicans* cells that were grown in YPD plates the day before, at multiplicity of infection (MOIs) of 1 and 5, and for different time points depending on the assays.

Environmental scanning electron microscopy (ESEM)

ESEM was performed as previously detailed.²⁵ After macrophage interaction with *C. albicans*, cells were washed in PBS containing 2.5% paraformaldehyde for 1 h at room temperature. They were incubated in 2% osmium tetroxide for 1 h and then in 2% tannic acid for 1 h. Cells were dehydrated in ethanol. They were examined at the FEI INSPECT microscope at the Museo Nacional de Ciencias Naturales (Madrid, Spain).

Cytokine determination

For cytokines measurements, macrophages from the THP-1 cell line were incubated with or without *C. albicans* cells at an MOI of 1 for 3, 6 and 8 h. As a positive control, macrophages were treated with lipopolysaccharide (LPS; 100ng/ml). Supernatants from untreated, LPS- or *Candida*-treated THP-1 macrophages were tested for cytokine production by ELISA using matched paired antibodies against different interleukins: IL-1 β , IL-6, IL-12p40 and TNF- α (Immunotools), according to manufacturer's instructions. Cytokine production was measured in three independent macrophage preparations.

***C. albicans* phagocytosis assay**

C. albicans yeast cells were pre-labelled with 1 μ M Oregon green 488 (Molecular Probes) in the dark with gentle shaking at 30°C for 1 h. THP-1 macrophages were differentiated in 18-mm glass sterile coverslips placed into 24-well plates and confronted with the yeast cells at a MOI of 1, at 37°C and 5% CO₂. Interaction was stopped after 45 min, 1.5 h and 3 h, and cells were then washed with ice-cold PBS and fixed with 4% paraformaldehyde for 30 min. To distinguish between internalized and attached/non-ingested yeasts, *C. albicans* cells were counterstained with 2.5 M Calcofluor white (Sigma) for 15 min in the dark. After several washes, coverslips were mounted with specific mounting medium (Southern Biotech). The number of ingested cells (green fluorescence) and adhered/non-ingested (blue fluorescence) were calculated by fluorescence microscopy.²⁶ Three different replicates with two different slides were prepared for each time point. At least 500 *C. albicans* cells were scored per slide, and results were expressed as the percentage of yeast cells internalized by macrophages.

Macrophage cell damage assay

In order to evaluate the *C. albicans* damage in the THP-1 cell line macrophages, the cytotoxicity detection kit (Roche) was used. This assay is based on the measurement of lactate dehydrogenase (LDH) activity released from the cytosol of damaged cells. Macrophages were cultured in 24-well plates as stated above, and *C. albicans* cells were incubated with them in a MOI of 1 and 5 at 37°C and 5% CO₂. The selected time points of measurements were 3 and 6 h. After these time points, the supernatants of the cells were removed for LDH measurement. The assay was performed according to manufacturer's instructions.

Macrophage cell line culture and SILAC labelling

THP-1 monocytes were grown in DMEM containing 10% dialyzed fetal bovine serum (FBS): i.e., either in light DMEM, containing 100 mg/l unlabeled L-arginine (Arg0) and 50 mg/l L-lysine (Lys0), or in heavy DMEM, containing 100 mg/l Arg6 (Silantes, ¹³C labelled Arginine · HCl) and 50 mg/l Lys6 (Silantes, ¹³C6 labeled L-Lysine · HCl). After 5 cell doublings, protein lysates of the macrophage cells were analyzed by MS to ensure that all proteins were labelled. Differentiation of monocytes into macrophages was triggered by the addition of PMA. Approximately, 20x10⁶ cells were plated in 150-mm culture dishes and 30 ng/ml PMA was added, cells were incubated for two days to achieve complete differentiation. PMA was removed by washing the cells with light and heavy DMEM medium, respectively.

Fungal infection for shotgun quantitative proteomics

C. albicans cells were counted using the Neubauer chamber, and 20x10⁶ cells were incubated with the macrophages (MOI of 1) for 3 h. In order to diminish the possible effect of the labelling procedure, in two biological replicates control macrophages were

labelled with light DMEM and macrophages upon interaction were labelled with heavy DMEM, while in the other two biological replicates this labelling was switched over. The extracted proteins came from the same number of macrophage cells in control and interaction conditions. In each experiment, both labelled and unlabeled lysates were mixed in protein concentration ratios of 1:1.

Preparation of the protein samples for shotgun proteomics

Cell lysis

After the incubation time, cells were washed twice with ice-cold PBS, and 1 ml of cold modified radioimmunoprecipitation assay (RIPA) lysis buffer (150 mM sodium chloride; 50 mM Tris-HCl pH 7.5; 1% NP40; 0.25% sodium deoxycholate; proteases inhibitors (1:1000, Pierce™); 1 mM sodium orthovanadate; 5 mM sodium fluoride; 5 mM β-glycerolphosphate and 5 mM sodium pyrophosphate) was added. Cells were scrapped thoroughly. Then, the cell lysate was placed on ice for 5 min, vortexed for another 5 min, and centrifuged at 15,000 rpm for 10 min and 4°C. The supernatant, containing the macrophage protein extract, was removed and transferred to a new tube. Protein concentration was measured using the Bradford assay.

Kinase enrichment with ATP probes

Protein lysates were enriched in kinases using ActivX desthiobiotin ATP probes (Thermo Scientific), according to manufacturer instructions with some alterations. Briefly, protein lysates were desalted using Zeba spin desalting columns to remove endogenous ATP. Then, lysates were eluted in reaction buffer and supplemented with protease inhibitors. Protein concentration was determined again by the Bradford assay. For labelling with the ATP probes, 2 mM MgCl was added to 2 mg of protein lysate and

1
2
3 incubated with 20 μ M of ActivX probe in a final volume of 500 μ l for 30 min at room
4
5 temperature with constant mixing. Then, 500 μ l of 12 M urea in lysis buffer were added
6
7 to the lysate to stop the reaction. Samples were then incubated with 125 μ l of high-
8
9 capacity streptavidin agarose resin for 1.5 h at room temperature with constant mixing.
10
11 Beads were collected by centrifugation at 1000g for 1 min and washed twice with 4 M
12
13 urea in lysis buffer. Finally, proteins were eluted by adding Laemmli reducing sample
14
15 buffer and boiling for 5 min.
16
17
18
19
20

21 **In-gel digestion**

22
23 Samples in Laemmli sample buffer were loaded into a 1.5 mm thick SDS-PAGE gel
24
25 with a 4% stacking gel casted over a 10% resolving gel. The run was stopped as soon as
26
27 the front entered 3 mm into the resolving gel so that the whole proteome became
28
29 concentrated in the stacking/resolving gel interface. Bands were stained with colloidal
30
31 Coomassie Brilliant Blue staining. Gels were cut into 12 to 15 slices for protein
32
33 digestion.²⁷ In-gel digestion was carried out as described.²⁸ Briefly, gel slices were cut
34
35 into pieces of 1 mm³ in size and washed with water. Proteins were reduced with 10 mM
36
37 DTT in 25 mM ammonium bicarbonate for 30 min at 56°C and then alkylated with 55
38
39 mM iodoacetamide in 25 mM ammonium bicarbonate for 15 min at 30°C. Acetonitrile
40
41 (ACN) and vacuum centrifugation were applied to dry the gel pieces. They were then
42
43 rehydrated with 60 ng/ μ l trypsin (proteomics grade; Roche Applied Science) in 25 mM
44
45 ammonium bicarbonate for 45 min at 4°C. The trypsin solution was removed, and the
46
47 rehydrated gel pieces were overlaid with 25 mM ammonium bicarbonate. The digestion
48
49 was performed overnight at 37°C. After digestion, the supernatant was recovered.
50
51
52 Peptides were extracted from the gel pieces with 30% ACN and 0.1% trifluoroacetic
53
54
55
56
57
58
59
60

acid (TFA) for 30 min at room temperature. Peptides were desalted onto C18 OMIX cartridges and dried-down.

Sequential elution from immobilized metal affinity chromatography (SIMAC) for phosphopeptide enrichment

A total of 300 µg of the protein lysate enriched in ATP-binding proteins was used for phosphopeptide enrichment. Both immobilized metal affinity chromatography (IMAC) and titanium dioxide (TiO₂) chromatography were performed as previously described⁷ and summarized below.

For each 100 µg of peptides, 40 µl of iron-coated PHOS-selectTM metal chelate beads (Sigma-Aldrich) were used. Beads were washed twice in loading buffer (0.1% TFA and 50% ACN), and incubated with 500 µg of peptide mixture in loading buffer for 30 min at room temperature in vibrating shaker. Then, beads were packed in the constricted end of a 200 µl GELoader tip by application of air pressure with a syringe, forming an IMAC column. The flow-through was collected for further analysis by TiO₂ chromatography. The IMAC was then washed with loading buffer, which was added to the flow-through. Both monophosphorylated peptides and contaminating non-phosphorylated peptides were eluted using acidic elution solution (1%TFA and 20% ACN) and the multiply phosphorylated peptides were eluted using basic elution solution (0.5% ammonia). The IMAC flow-through and both eluents were dried in a vacuum concentrator. A TiO₂ microcolumn was prepared by stamping out a small plug of C18 material from a C18 extraction disk and placing the plug in the constricted end of a 200 µl GELoader tip. The TiO₂ beads were first suspended in loading buffer (1 M glycolic acid in 5% TFA and 80% ACN) and then mixed with the sample and incubated for 15

min with constant mixing. This mixture was centrifuged and 90% of the supernatant was removed to minimize the volume introduced in the microcolumn. The sample was applied to the tip and the TiO₂ column was packed by the application of air pressure with a syringe. The column was washed with loading buffer and subsequently with washing buffer (80% ACN and 5% TFA). The phosphopeptides bound to the TiO₂ microcolumn were eluted using 30 µl of 0.5% ammonia followed by elution using 1 µl of 30% ACN to elute phosphopeptides bound to the C18 disk. Then, the eluent was acidified by adding 5 µl of 100% formic acid and dried in the vacuum concentrator.

MS analysis

Peptides were trapped onto a C18 SC001 2-cm precolumn (Thermo-Scientific), and then eluted onto a NS-AC-11 dp3 BioSphere C18 column (75 µm inner diameter, 15 cm long, 3 µm particle size; NanoSeparations) and separated using a 140 min gradient (0-40% buffer B for 120 min; 40%-95% buffer B for 15 min, and 95% buffer B for 5min; buffer A: 0.1% formic acid/2%ACN; buffer B: 0.1% formic acid in ACN) at a flow-rate of 250 nL/min on a nanoEasy HPLC (Proxeon) coupled to a nanoelectrospray ion source (Proxeon). Mass spectra were acquired on a LTQ-Orbitrap Velos mass spectrometer (Thermo-Scientific) in the positive ion mode. Full-scan MS spectra (m/z 300–1,900) were acquired in an Orbitrap at a resolution of 60,000 at 400 m/z and the 15 most intense ions were selected for collision induced dissociation (CID) fragmentation in the linear ion trap with a normalized collision energy of 35%. Singly charged ions and unassigned charge states were rejected. Dynamic exclusion was enabled with exclusion duration of 30 s.

Protein/peptide identification and quantification

Mass spectra raw data files were searched against the SwissProt human database version 57.15 (20,266 protein entries) using MASCOT search engine (version 2.3, Matrix Science) through Proteome Discoverer (version 1.4.1.14; Thermo Fisher). Search parameters included a maximum of two missed cleavages allowed, carbamidomethylation of cysteines as a fixed modification, and oxidation of methionine, desthiobiotinylation of lysine, ^{13}C -arginine and ^{13}C -lysine as variable modifications. Precursor and fragment mass tolerance were set to 10 ppm and 0.8 Da, respectively. Identified peptides were validated using Percolator algorithm with a q -value threshold of 0.01. Peptide quantification from SILAC labels was performed with Proteome Discoverer v1.4 using node precursor ion quantification. For each SILAC pair, the area of the extracted ion chromatogram was determined and the “heavy/light” ratio computed. Ratios were normalized by the median of all peptides ratios in each biological replicate. Media and standard deviation were calculated for each peptide. Protein ratios were then determined as the median of all the quantified peptides belonging to a certain protein. The quantification was analyzed at the peptide level, and peptide ratios were manually evaluated. Peptides that presented discrepant values inside each protein were discarded as soon as this elimination did not change the trend of the ratio presented, and the standard deviation was improved. By this way, an increase in the coverage of the quantified proteins was achieved.

Regarding phosphorylation, the variable modification of phosphorylation (STY) was added for peptide identification. The PhosphoRS node was used to provide a confidence measure for the localization of phosphorylation in the peptide sequences identified with this modification. The phosphorylation sites were manually corrected based on the PhosphoRS localization probability for a given residue. The phosphorylation sites assigned with a localization percentage $<75\%$ were considered ambiguous. In addition,

1
2
3 if the percentage was >75% but different in the biological replicates were also
4
5 considered ambiguous. The phosphopeptides were treated similarly as in quantitative
6
7 analysis with the exception that the quantification was performed only at peptide level.
8
9
10 Mass spectra raw data files (both quantitative and phosphorylation files) were also
11
12 searched against the SwissProt human database for the discovery of possible missing
13
14 proteins.
15
16
17 To make our findings publicly available and accessible to the community, we have
18
19 deposited our dataset in ProteomeXchange Consortium via the PRIDE partner
20
21 repository with the dataset identifier PXD009938.
22
23
24
25

26 **Western blotting**

27
28 Protein lysates were obtained as stated above but without cell labelling, and used for the
29
30 proteomic validation assays. Forty µg of protein lysate were loaded in each well of a
31
32 10% SDS-PAGE gel and electrophoretically separated. After this, the proteins were
33
34 transferred onto nitrocellulose membranes (Hybond-ECL; GE Healthcare). The
35
36 membranes were blocked with 5% skinny milk in PBS for 2 h, and incubated with
37
38 primary antibodies, including anti-PRDX5 (Abcam) (1/125), anti-MEK2 (Cell
39
40 Signaling Technology) (1/500), anti-cleaved caspase-3 (Cell Signalling Technology)
41
42 (1/1000), anti Erk-1/2 (Cell Signaling Technology) (1/1000), or anti-Tubulin- α
43
44 (Serotec) (1/1000), anti P-Erk1/2 (Cell Signalling Technology) (1:1000) for 18 h at 4°C.
45
46
47 The membranes were washed 4 times with PBS containing 0.1% Tween-20 and
48
49 incubated with IRDye® secondary antibodies for 1 h (1/4000 IRDye 800CW goat anti-
50
51 mouse IgG, IRDye 680LT goat anti-mouse IgG, IRDye 800CW goat anti-rabbit IgG or
52
53 IRDye 680LT goat anti-rabbit IgG, as appropriate). Membranes were then washed four
54
55 times with PBS containing 0.1% Tween-20. Odyssey system (LI-COR ®) was used to
56
57
58
59
60

1
2
3 detect the fluorescence signals. Protein abundance was compared between control and
4
5 infected macrophages and values were given as arbitrary fluorescence units. Detection
6
7 of tubulin- α was used as a loading control.
8
9

10 11 12 **Selected reaction monitoring (SRM)** 13

14 The abundance of the protein NDKA was quantified using SRM. A proteotypic peptide,
15
16 which is a peptide unique to the target protein and easily detectable by mass
17
18 spectrometry was selected for protein quantification.²⁹ The selected peptide was
19
20 FMQASEDLLK because it was quantified in the shotgun approach and reached several
21
22 criteria necessary for SRM. These criteria were as follows: it should be proteotypic and
23
24 easy to synthesize and have moderate hydrophobicity. Unpurified isotopic labelled
25
26 peptide was obtained from JPT Peptide Technologies GmbH. Skyline software (Seattle
27
28 Proteome Center) was used for the optimization of SRM methodology and for the
29
30 analysis of the resulting MS data. Protein lysates were obtained as stated above, but
31
32 without labelling the cells, enriched using ATP-probe and digested as previously shown.
33
34 These SRM experiments were performed on a Q-TRAP ® 5500 LC-MS/MS system
35
36 (AB Sciex). Both peaks from the endogenous and heavy peptides were evaluated
37
38 manually. The area ratio (endogenous peptide area divided by heavy peptide area) was
39
40 compared in both conditions (control and interaction). Three biological replicates and at
41
42 least 2 technical replicates were performed.
43
44
45
46
47
48
49
50

51 **Bioinformatic analysis of the differentially abundant proteins** 52

53 Gene ontology (GO) enrichment analysis was performed using Genecodis
54
55 (<http://genecodis.cnb.csic.es/>)³⁰⁻³² and Panther (<http://pantherdb.org/>) web tools. For GO
56
57 analysis, statistical significance was set at p -value < 0.05. STRING software version
58
59
60

10.0 (<http://string-db.org>) was used for the study of the protein-protein interactions.³³ Ingenuity Pathway Analysis (IPA) (QIAGEN Bioinformatics) was used both for the prediction of possible upstream regulators and for network analysis.

Quantitative RT-PCR

RNA was isolated using the microRNeasy mini kit (QIAGEN) according to the manufacturer's protocol. Samples were quantified by Nanodrop 2000C (Thermo Fisher Scientific) and the presence of small RNA was confirmed using the Bioanalyzer 2100 (Agilent). Total RNA was reverse transcribed using Taqman microRNA reverse transcription kit (Thermo Fisher Scientific) and 10 ng of total RNA from each sample. Quantitative real time polymerase chain reaction (RT-PCR) for miRNA was performed using TaqMan microRNA assays (Thermo Fisher Scientific) following the manufacturer's instructions. U6 snRNA was used as an endogenous control, and the microRNAs (miRNAs) analyzed were mmu-miR-124a, hsa-miR-146a, hsa-miR-155 and hsa-miR-21.

Statistical analysis

In the SILAC experiment, the protein abundance ratio was the amount of protein in the macrophages upon interaction with *C. albicans* divided by the amount of protein in the control macrophages (without interaction with *C. albicans*). The log₂-transformed mean macrophage protein abundance ratios upon *C. albicans* interaction were stratified into seven quantiles according to their distribution in the sample: Q₁ (the lower extreme values), Q₂ (the lower outlier values), Q₃ (the smaller values that extended to 1.5 times the lower quartile or 25th percentile), Q₄ (the interquartile range, *i.e.* 25th to 75th percentiles), Q₅ (the larger values that extended to 1.5 times the upper quartile or 75th

percentile), Q_6 (the upper outlier values), and Q_7 (the upper extreme values). The first and seventh quantiles comprised those macrophage proteins that had the lowest and highest relative abundance ratios, respectively, upon interaction with *C. albicans*. The same analysis was performed for phosphorylated peptides. All quantitative data were presented as mean \pm standard deviation (SD).

For Western blotting, cytokines and SRM assays, comparisons between two groups were performed by the Student's t-test. Statistical significance was defined as * for p -value <0.05 , ** for p -value <0.001 and *** for p -value <0.0001 . Three biological replicates were performed for Western blotting and SRM-based validation assays, with exception of cleaved-caspase Western blotting that was performed with two biological replicates.

The mi-RNA expression level was calculated using $\Delta\Delta Ct$ formula.³⁴ The results were represented using the relative fold-change expression compared to the control, where the control values were considered a value of 1. Four biological replicates were used in this assay.

For all the assays, conditions were tested with Student's t-test. A p -value lower than 0.05 was considered statistically significant.

RESULTS

THP-1 macrophages and *C. albicans* co-culture

The optimal conditions were set up to characterize differentially abundant proteins from human macrophages upon *C. albicans* infection. The damage of *C. albicans* in the THP-1 macrophages was evaluated by lactate dehydrogenase measurements in two MOIs (Figure 1A). *C. albicans* produced more damage to THP-1 cells in a MOI of 5 than in a MOI of 1, as expected. Damage increased over time of incubation at both MOIs. A MOI

of 1 was selected due to the lowest observed damage. After MOI selection, phagocytic activity was measured. *C. albicans* cells ingested or associated with macrophages were discriminated using differential staining with Oregon green and calcofluor white. THP-1 macrophages showed an increase in their phagocytic activity over time (from 45 min to 3 h), almost 70% of *Candida* cells being engulfed after 3 h of interaction (Figures 1 B and C). Taking into account these results and some studies performed before by our laboratory,^{7-8, 26, 35} a MOI of 1 and the time point of 3 h were the conditions used for the quantitative proteomic assay. With these conditions, it was assured that 70% of *C. albicans* cells were engulfed and most macrophages were viable. Macrophage - *C. albicans* co-culture in the selected conditions was visualized by ESEM (Figure 1D). As shown, after 3 h of interaction *C. albicans* cells were already in hypha form and at different stages of interaction with the macrophage.

Quantitative proteomic analysis of macrophage proteins after interaction with *C. albicans*

A quantitative shotgun proteomic approach using SILAC and LC-MS/MS was used to study the changes in the abundance of macrophage proteins enriched after using the ActivX desthiobiotin ATP probes upon interaction with *C. albicans* cells during 3 h at a MOI of 1. Protein lysate was enriched in ATP-binding proteins and samples were analyzed by LC-MS/MS. Four biological replicates and two technical replicates of each were analyzed by MS and a schematic workflow of the experimental procedure is reflected in Supplementary Figure 1. A total of 1043 proteins were identified, corresponding to 710, 664, 664 and 709 proteins in each replicate, respectively (Supplementary Table 1 and Supplementary Figure 2). A total of 547 non-redundant proteins were quantified in at least two biological replicates with a SD <0.3

(Supplementary Table 2). The molecular functions enriched on the 547 quantified proteins were mainly protein binding (271 proteins), nucleotide binding (203 proteins) and ATP binding (136 proteins). Furthermore, the total number of quantified proteins was enriched in 10 major biological processes, such as gene expression (87 proteins), cellular protein metabolic process (76 proteins), and translation (65 proteins). Regarding the cellular component, most of the proteins were located in cytoplasm (341 proteins), followed by nucleus (205 proteins), and mitochondria (105 proteins) (Supplementary Figure 3).

The macrophage proteins extracted using the ActivX desthiobiotin ATP probes showed a very homogeneous abundance ratio. After stratification of protein abundance ratios into quantiles according to their distribution upon interaction with *C. albicans*, we found that 4 and 9 proteins had the higher and lower extreme abundance ratios, whereas 18 and 28 proteins had the higher and lower outlier abundance ratios, respectively (Supplementary Figure 4 and Table 1). Out of these 59 differentially abundant proteins, 12 were annotated as ATP binding proteins. GO term enrichment analysis showed that the more abundant proteins were involved in gene expression and RNA metabolic process, whereas the less abundant proteins were associated with proteolysis, apoptotic processes and endocytosis, among others. Both, the more and less abundant macrophage proteins, were related to the same molecular functions, such as protein binding and nucleotide binding. Furthermore, the more abundant proteins were associated with RNA binding or peroxiredoxin activities, while the less abundant proteins were related to ATP binding or peptidase activities. Both the more and less abundant proteins were enriched in the cytosol and mitochondrion GO terms (Figure 2). The more abundant mitochondrial proteins during interaction included SLC25A24 and PRDX5, which are important in the response to oxidative stress³⁶⁻³⁷.

The analysis of known and predicted protein-protein interactions was also performed with these 59 differentially abundant macrophage proteins upon *C. albicans* interaction (Figure 3). Forty-five protein-protein associations were found based on known or predicted interactions. Different clusters of protein associations were observed. A cluster enriched in proteins that were more abundant during *C. albicans* interaction was involved in protein synthesis. The group of proteins that were less abundant was very heterogeneous in molecular function GO terms and included a cluster of proteins involved in proteolysis and endocytic traffic. Other clusters containing both the more and less abundant proteins were related to RNA processing and apoptosis.

Analysis of the quantified proteins annotated as ATP-binding proteins

A comparison between all the proteins annotated as ATP binding in Uniprot database and the proteins quantified in this study was performed. From the 1482 proteins annotated with the ATP binding term, 137 were also present in the 547 proteins quantified in this study (Supplementary Table 2). This means that approximately 25% of all the quantified proteins were annotated as “ATP-binding”. A list of all ATP binding proteins quantified and grouped by protein family is represented in Table 2. Among them, 4 proteins (MAP2K2, KSYK, DDX21 and SYCC) were more abundant during the interaction, and 8 proteins (PRS10, SYIM, STK3, OAS3, MAP3K2, RTCB, NDKA and SRPK1) were less abundant after the interaction. In this group of differentially abundant ATP-binding proteins, 6 were kinases (MAP2K2, SYK, STK3, MAP3K2, NDKA and SRPK1). The group with more quantified proteins was the protein kinase superfamily, with 24 quantified protein kinases (Table 2). GO analysis on molecular function showed an over-representation of terms related to ATP binding (like nucleotide binding), ATPase activity and kinase activity (Supplementary Table 3).

Regarding the GO analysis on cellular component, in addition to cytosol that was already expected, an over-representation on terms related to chaperonin-containing T complex, proteasome, mitochondria or extracellular vesicles was also observed. Concerning the GO analysis on the biological processes, there was an over-representation in terms such as regulation of protein localization to Cajal bodies (which are implicated in mRNA processing),³⁸ tRNA aminoacylation for protein translation, protein folding, regulation of protein stability, and positive regulation of cellular biosynthetic process. There was also an over-representation on processes related to immune response, such as regulation of cellular response to stress and activation of innate immune response.

Phosphoproteomic analysis of macrophage proteins after interaction with *C. albicans*

The fraction enriched in ATP-binding proteins from all 4 biological replicates was further subjected to phosphopeptide enrichment. A total of 85 phosphopeptides were quantified in at least two biological replicates and with a SD < 0.3 and are listed in Supplementary Table 4. In some cases two or more phosphopeptides were quantified for the same phosphorylation site (phosphosite). Therefore, 85 phosphopeptides corresponding to 70 phosphosites and 56 proteins were quantified. According to the phosphorylation probabilities given by the Proteome Discoverer software, the phosphosites were considered ambiguous or assigned to a specific amino acid (serine, threonine and tyrosine). Sixty-one percent of the phosphosites were phosphorylated in serine and 33% were ambiguous, whereas phosphothreonine and phosphotyrosine were less represented (3% each). Out of the 56 phosphoproteins, 25 (approximately 36%) are from proteins that were annotated as ATP-binding proteins in UNIPROT database and

12 (21.4%) as kinases. Out of the 85 quantified phosphopeptides, 5 phosphopeptides (each one belonging to a single protein) were differentially abundant during macrophage interaction with *C. albicans* (Table 3 and Supplementary Figure 5). From this, 2 phosphopeptides belonging to PRKAA1 and CLN6 were more abundant during interaction, whereas 3 phosphopeptides belonging to PI4K2A, SRC and PRKCD were less abundant. Their mass spectra are shown in Supplementary Figure 6.

Protein validation

To confirm the quantitative MS data, Western blot analysis using antibodies to MAP2K2, PRDX5 and ERK1/2, and SRM of NDKA were performed. There was a significant increase in MAP2K2 (ratio between interaction and macrophages control of 1.6) and PRDX5 (ratio of 2.1) abundance during macrophage interaction with *C. albicans* cells in line with MS data (Figures 4A and 4B). Because MAP2K2 is a kinase that acts upstream ERK1/ERK2 kinases and is important for several cellular processes,³⁹ we also validated this protein by Western blotting. No significant differences in ERK1/2 abundance upon interaction were detected, confirming our proteomic data (Figure 4C). In addition, phosphorylation of ERK1/2 was also evaluated and no increase in phosphorylation was observed (Supplementary Figure 7). For SRM validation, the correspondent isotopic labelled peptide was ordered, and a calibration curve was performed (see Supplementary Figure 8 and Supplementary Table 5). The quantification of this peptide confirmed the decrease in the amount of NDKA (ratio of 0.24) (Figure 4D and Supplementary Table 5).

Macrophage cell death mechanisms and pro-inflammatory response

Apoptosis was one of the biological processes enriched in the group of less abundant proteins. A closer look showed an increase in PRDX5, SLC25A24 and ADT2, which are anti-apoptotic proteins, and a decrease NDKA, ACTN4 and STK3, which are pro-apoptotic or anti-survival proteins^{36, 40-44}. In order to functionally validate these results, the apoptotic status of THP-1 macrophages after interaction with *C. albicans* was assayed by measuring caspase-3 activation by cleavage. Cells were incubated with staurosporine (as a positive control of apoptosis) and with *C. albicans* cells (at a MOI of 1 for 3 h). Activated caspase-3 was assayed by Western blotting with cell lysates and a band corresponding to the activated caspase 3 was observed in the positive control but not in macrophage-*C. albicans* interaction at 3 h (Figure 5A). As cleaved caspase 3 is a hallmark of apoptosis,⁴⁵ this result suggests that apoptosis was not present in these conditions. In congruence with our results, it was previously described by others that *C. albicans* triggers pyroptosis during the first 6 to 8 h of interaction with macrophages,⁴⁶ we checked IL-1 β secretion (which is secreted after caspase-1 activation)⁴⁷. IL-1 β was significantly more secreted in macrophages after interaction with *C. albicans* (Figure 5B). Furthermore, as pyroptosis is an inflammatory mechanism of cell death,⁴⁷ other pro-inflammatory cytokines were evaluated. As depicted in Figures 5C and 5D, there was more secretion of pro-inflammatory cytokines IL-12p40 and TNF- α upon interaction with *C. albicans*.

To further predict potential upstream regulators implicated in the macrophage inflammatory response, the 59 differentially abundant proteins were also analyzed using the IPA software. Fifteen upstream regulators presented an activation z-score between -2 and 2 and a *p*-value of overlap < 0.05, which included CD3 complex, cytokines (oncostatin M (OSM), IL5 and IL6), proteins (KRAS; VEGFA; MAPK1; ESR1), miRNAs (miR-124-3p and miR-21), transcription regulators (MYCN, MYC and TP53),

transmembrane receptor CD28 and rapamycin-insensitive companion of mTOR (RICTOR) (Figure 6A). The higher or lower z-score showed the higher probability of activation or inhibition of the upstream regulator, respectively. The IL-6 gene was predicted to be inhibited. This prompted us to assay the secretion of this cytokine at different time points (3h, 6h and 8h) of THP-1 macrophage-*C. albicans* interaction. This cytokine was not secreted after interaction with yeast cells (Figure 6B), indicating that this gene may not be expressed under these conditions. Due to the recent evidences in the implication of miRNAs (miR) in the regulation of innate immune response,⁴⁸ we also evaluated the possible activation miR-21 and miR-124 (two miRNAs that were predicted to be activated; Figure 6A). The expression levels of miR-21 and miR-124 were evaluated together with miR-146 and miR-155 (which are activated after treatment with LPS in THP-1 cells²⁴ and also after interaction with heat inactivated *C. albicans* cells⁴⁹⁻⁵¹). MiR-21 and miR-124 were slightly, but not statistically significant, activated after treatment with LPS, and showed no significant activation in response to *C. albicans* (Figures 7A and 7B, respectively). Regarding miR-146 and miR-155, they were activated in response to LPS (Figures 7C and 7D, respectively), but also no significant activation in response to live *C. albicans* cells after 3 h and 6 h of interaction was observed.

DISCUSSION

The current approaches to decrease fungal infections are still limited and are mainly pathogen-directed therapeutics.⁵² In this way, the study of the immune response may give us new clues on how this pathogen can be killed, and consequently improve the currently available therapeutic approaches. Furthermore, increasing efforts are being done to develop specific ways to modulate the immune system as new therapeutic

strategies.⁵³⁻⁵⁴ Macrophages are cells from the innate immune system that play an important role in the host response and elimination of pathogens.⁴ ATP-binding proteins are essential in several cellular processes including cell signaling, differentiation apoptosis and others.²¹ Despite this fact, proteomic studies of this group of proteins are generally difficult because they are at low abundance in the cell. In this way, we decided to perform a selective enrichment in ATP-binding proteins with an ATP probe¹⁶ in order to get more information on this subproteome. Taking advantage of this approach, a quantitative proteomic study of human macrophage proteins after interaction with *C. albicans* cells was carried out in this work and allowed the quantification of proteins that could be involved in the response to this pathogen. In this study, THP-1-derived macrophages were incubated with *C. albicans* cells during 3 h and a MOI of 1. PMA was used for the differentiation of THP-1 monocytes. The up-regulation of specific genes during the differentiation process might overwhelm mild effects of specific stimuli. Nevertheless, this cell line was described to be very close to primary human cells and used previously for the study interaction with pathogens.⁵⁵⁻⁵⁹ At 3 h of interaction, a reduced damage was ensured, so 70% of the macrophages were not impaired and around 70% of yeast cells were engulfed by the macrophages. This evaluation of human macrophage interaction with *C. albicans* is in agreement with our previous studies with murine macrophage cell lines and was peremptory to select the ratio and time of incubation.^{7, 26}

Enrichment in ATP binding macrophage proteins

In this study, 547 non-redundant macrophage proteins were quantified, approximately 25% of which were annotated in Uniprot as “ATP-binding” proteins. Proteins that were quantified and not annotated as ATP binding proteins could be either proteins that were

interacting with the ATP binding proteins or proteins that resulted from unspecific binding with the probe. The protein family with more quantified ATP-binding proteins was the protein kinase superfamily (with 24 quantified protein kinases). Out of these 24 protein kinases, 13 proteins were included in the Ser/Thr (STE) protein kinase family. The preference to this protein kinase family was previously observed by Lemeer and co-workers.⁶⁰ They performed a comparison between two enrichment methods (ATP-affinity probe and kinobeads). They found a higher number of tyrosine kinases enriched with kinobeads, while more kinases from the STE kinase group were enriched with the ATP affinity probe. They detailed that small molecules inhibitors immobilized in kinobeads were originally developed to target tyrosine kinases, whereas the reaction mechanism of the ATP probe was distinct.⁶⁰

Differentially phosphorylated macrophage peptides after interaction with *C. albicans*

In addition to protein abundance, phosphorylation information can significantly enhance our knowledge on the involvement of macrophage ATP-binding proteins in different cellular mechanisms during interaction with pathogens. Furthermore, an important group of ATP binding proteins include kinases which are known to be highly phosphorylated in cell signaling processes where they are implicated.⁶¹ Although few phosphorylation results were obtained, 5 differentially abundant phosphopeptides were found and 4 of them were key kinases in cell signaling pathways. This means that type of enrichment in ATP binding proteins, coupled with the new and more potent mass spectrometers, can be a useful tool for the study of kinase phosphorylation sites. Regarding the more abundant phosphopeptides during macrophage-*C. albicans* interaction, they corresponded to CLN6 and PRKAA1. Neuronal ceroid lipofuscinosis

are lysosomal storage disorders and mutation in CLN genes are the cause of this disease. Among them, CLN6 is involved in endocytosis of lysosomal proteins.⁶² However, little is known about this protein in other contexts. PRKAA1 presented the phosphopeptide that showed the highest increase in abundance during macrophage interaction. This protein is a sensor of energy status that maintains cellular energy homeostasis.⁶³ The phosphorylation of Thr183 is known to activate this kinase.⁶⁴⁻⁶⁵ It was previously shown that the activation of this kinase was implicated in phagocytosis of both bacteria⁶³ and fungi (like the pathogen *Cryptococcus neoformans*)⁶⁵. Phosphorylation of AMPK α in Ser487/491 was found to reduce AMPK activity⁶⁶. In this study, the quantified AMPK α phosphopeptide had several possible phosphosites assigned: Ser494, Ser496 and Tyr500. A search in Phosphosite Plus[®] showed that the phosphorylation of Ser496 would be responsible for the inhibition of the enzymatic activity. However, further studies would be needed to know the cellular effects of this phosphopeptide.

The less abundant phosphopeptides during macrophage *C. albicans* interaction belonged to PRKCD, SRC and PI4K2. PRKCD and SRC are known to be activated after macrophage receptor recognition of *C. albicans* PAMPs.^{4, 67} During this study, both phosphopeptides were found to be less abundant during interaction. SRC was found to be less phosphorylated in the activation site (Tyr419) during interaction. Due to its implication in several fundamental processes, including cell differentiation, proliferation, migration and survival⁶⁸ in addition to its involvement in the inflammatory process,⁶⁹ deeper analysis and time course experiment would be needed to further explain these results. In any case, SRC is one of the primary kinases to be activated after receptor engagement,⁴ it is plausible that after 3 hours of incubation this kinase is no longer phosphorylated, once the signaling cascades are already activated.

PI4K2A was previously described to be involved in the correct endocytic traffic.⁷⁰ Interestingly, the quantitative proteomic results showed that two proteins implicated in endosomal trafficking, RAB7A and TFR1, were less abundant during macrophage interaction with *C. albicans*.⁷¹⁻⁷³ These data together with the fact that our group previously supported the model where *C. albicans* evade trafficking to lytic compartments in murine macrophages³⁵ make us hypothesize that also during this experiment *C. albicans* may be modulating phagosome maturation. This phenomenon was previously observed during macrophage-*Mycobacterium tuberculosis* interaction.⁷¹⁻⁷²

Mitochondrial proteins and oxidative stress response

In general, the overall quantification of the ATP binding proteins subproteome enriched with this method presents slight changes in its abundance upon interaction with *Candida*. This may be due to the pre-activation with PMA needed to differentiate monocytes into macrophages. Macrophages are phagocytic cells that produce and release reactive oxygen species (ROS) in response to phagocytosis.⁷⁴ Two mitochondrial proteins involved in response to oxidative stress (PRDX5 and SLC25A24) were found to be more abundant upon interaction with *C. albicans*. PRDX5, a protein that protects cells from DNA damage and inhibits stress-induced apoptosis,⁴⁰ was previously shown to be more abundant in LPS-treated macrophages.⁷⁵ We validated the increase in its abundance using Western blot. SLC25A24 may also play a role in protecting cells against oxidative stress-induced cell death.³⁶ Another group previously observed significant changes in redox-related proteins implicated in oxidative burst in order to kill intracellular mycobacteria. They observed an increase in the abundance of several proteins that counteract the effect of oxidative stress.⁷⁶ We

can hypothesize that the higher abundance of proteins that neutralize the oxidative burst may be a host-driving response to protect itself from the ROS production because after three hours of interaction *Candida* cells are already producing hypha which promotes phagolysosome rupture. Nevertheless, we may not discard the possibility that it can also be a pathogen-driven response (to reduce the production of ROS and decrease the killing power of the macrophages). In addition to being of highly importance to ATP production and electron transport chain, mitochondria were recently implicated in innate and adaptive immunity.⁷⁷ Knowing this, we took a more careful look to the quantified proteins located in the mitochondria. In general terms, we observed an increase in the mechanisms that protect cell against oxidative stress as well as transport of ATP to the cytoplasm. This behavior is understandable once macrophages increase the amount of ROS to kill *C. albicans*. So, the increase in abundance of these proteins could play a role in the phagocyte protection against the produced oxidative stress. Furthermore, the higher demand of metabolites and proteins could explain the need of the mitochondria to increase the transport of ATP to the cytosol.

Host proteins involved in mRNA processing and translation

HNRNPCL1, a heterogeneous nuclear ribonucleoprotein, was the protein with the highest differential abundance in our study. HNRNPs are operationally defined as proteins that bind to RNA⁷⁸ and are responsible for packing and stabilizing them.⁷⁹ Little is known about HNRNPCL1. Nevertheless, HNRNPC was one of the first HNRNPs found to be involved in RNA splicing.⁸⁰ The depletion of these C proteins from splicing extracts abolished splicing activity. Thus, we can hypothesize that HNRNPCL1, which has a 90.8% identity with HNRNPC, may have a similar role to HNRNPC. Interestingly, an increase in the abundance of several HNRNPs was

previously observed in THP-1 cells infected with *Leishmania* parasites.⁵⁵ String analysis showed a cluster of (more and less abundant) proteins involved in RNA processing. Further validation and functional studies are necessary to define the role of splicing proteins in the macrophage response to *C. albicans*.

Another group of differentially more abundant proteins were ribosomal proteins (RPS26, RPL3, RPL9 and DDX21). A higher abundance of these proteins may be a mechanism of the host cells to meet the increasing need of proteins to fight the fungal infection. In line with the upregulation of the protein synthesis process, a decrease in the abundance of proteins involved in proteolysis (MMP9, LAP3, DPP7 and DLD) was observed.

Macrophage cell death and inflammatory response to *C. albicans*

We also observed enrichment of proteins related to apoptosis. We found that anti-apoptotic signals were up-regulated in THP-1 macrophages infected with *C. albicans*, as compared to pro-apoptotic signals. Knowing that caspase-3 is one of the executioners of apoptosis, we measured its cleavage by Western blotting and no cleavage of this protein was observed after THP-1 macrophage interaction with *C. albicans*.⁸¹ A previous work from our research group reported no apoptosis in RAW 264.7 macrophages incubated with *C. albicans*.⁷ The way by which macrophages activate cell death mechanisms as a consequence of uptaking *C. albicans* cells has been studied previously. Uwamahoro and co-workers showed that *C. albicans* triggers pyroptosis during the first 6 to 8 h of interaction.⁴⁶ In concordance to our results, they observed no evidence of activation of caspase-3 by *C. albicans* early post-infection. More recently, another group suggested that neutralization of the phagosome by *C. albicans* is an important signal in activating the macrophage inflammasome.⁸² The pro-inflammatory cytokine IL-1 β is released as a

1
2
3 result of *C. albicans* driven NL3PR inflammasome activation and has been used as a
4
5 measurement of pyroptotic cell death in the immune cell in response to microbial
6
7 pathogens.⁸²⁻⁸⁴ An increase of this cytokine was observed after 3 h of interaction with
8
9 *C. albicans*, suggesting that pyroptosis could be activated in response to *C. albicans*.
10
11 However, further validation confirming caspase-1-dependent IL-1 β release would be
12
13 needed to confirm this phenomenon in this cell line. We were also interested in knowing
14
15 whether other pro-inflammatory cytokines were secreted. Both TNF- α and IL-12 were
16
17 significantly more secreted after 3 h of interaction with *C. albicans*. This pathogen is
18
19 known to trigger a pro-inflammatory response of the macrophages, including the release
20
21 of these cytokines.⁸⁵ The IPA software was used to predict upstream regulators of the
22
23 pro-inflammatory response. This analysis is based on prior knowledge of expected
24
25 effects between transcriptional regulators and their target genes that are stored in
26
27 Ingenuity® Knowledge Base (taking into account previously published datasets derived
28
29 from different animal models).⁸⁶ This analysis suggested 15 potential regulators of gene
30
31 expression for the genes encoding the proteins identified in this. In order to validate
32
33 some of these predictions, we evaluated the secretion of IL-6 and the activation of miR-
34
35 21 and miR-124. The analysis performed by IPA presented a negative activation z-score
36
37 of IL-6 and in accordance with this, no secretion of IL-6 was observed. IL-6 is a pro-
38
39 inflammatory cytokine and was previously observed not to be secreted after interaction
40
41 with *C. albicans*.^{8, 87} Recently, mi-RNAs have been implicated in immune response,
42
43 particularly as post-transcriptional regulators of the inflammatory response. There are
44
45 several mi-RNAs that regulate TLR signaling pathways. Monk and co-workers showed
46
47 that miR-155, miR-146a, miR-146b, miR-125a and miR-455 were upregulated after
48
49 treatment with LPS and after interaction with heat killed *C. albicans* cells.⁵¹ Another
50
51 group was interested in the impact of *C. albicans* cell morphology (heat killed yeast and
52
53
54
55
56
57
58
59
60

hyphal cells) in the differential regulation of host mi-RNAs.⁵⁰ They suggested that dectin-1 may be orchestrating miR-155 up-regulation in a Syk-dependent manner. Since our proteomic approach was performed with live *C. albicans* cells, we investigated the differential mi-RNAs regulation upon interaction with live *Candida* cells. The selected mi-RNAs were those predicted to be up-regulated by IPA (miR-21 and miR-124) and those found to be induced upon LPS activation and after interaction with heat killed *C. albicans* cells (miR-146 and miR-155).⁴⁹ Because we used live cells, our time points were shorter than others. We found that miR-21 and miR-124 were slightly, but not significantly, up-regulated after treatment with LPS. After interaction with *C. albicans*, none of these mi-RNAs were statistically significant upregulated. In our conditions and time points, the results were different from the predicted by IPA. Both miR-146 and miR-155 were confirmed to be upregulated after macrophage treatment with LPS. This was in concordance with the other work where miR-146 was shown to be involved in the mechanism of negative feedback regulation of TLR.⁴⁹ Interestingly, after macrophage interaction with live *C. albicans* cells, no upregulation of these mi-RNAs was observed at these time points. Although longer time points would be needed to determine whether this behavior is maintained, we can hypothesize that these miR were not yet activated because macrophages might need a much higher pro-inflammatory response to kill *C. albicans*, or because this fungus may be inducing a longer pro-inflammatory response to destroy the macrophage. The inflammatory effect induced by live *C. albicans* cells was previously suggested by our group as virulence trait responsible for tissue damage in the host.^{7, 88} It is important to underscore the need of follow-up studies to reveal whether this is a host-driven or pathogen-driven mechanism.

CONCLUDING REMARKS

The ATP-binding enrichment together with the SILAC proteomic and phosphoproteomic approach revealed new insights into the possible remodeling processes altered upon macrophage interaction with this human pathogen. A summary of these processes is depicted in Figure 8. Interestingly, an increase in the abundance of proteins involved in protein synthesis was observed together with an increase in the abundance of mitochondrial proteins responsible for macrophage response against oxidative stress. Regarding the cell death mechanisms, anti-apoptotic signals were more abundant than pro-apoptotic signals, in line with the lack of caspase-3 cleavage during interaction. A high pro-inflammatory response of the macrophage was observed, by the secretion of TNF- α and IL-12 cytokines together with the lack of activation of some mi-RNAs involved in the control of the pro-inflammatory response. Phosphorylation together with quantitative proteomic results suggested a possible reduction of the endosomal trafficking inside the macrophage. This study constitutes a valuable way to better understand cellular mechanism of response or readjustments and is important for the future development of new therapeutic approaches.

FIGURE LEGENDS

Figure 1. THP1 macrophage interaction with *C. albicans* cells. (A) Lactate dehydrogenase cytotoxicity assay to measure the damage of *Candida* cells in THP1 macrophages after 3h and 8h of interaction with *C. albicans* cells and at a MOI of 1 and 5. (B) Fluorescence microscopy images of THP1 macrophages exposed to labeled *C. albicans* strain SC5314 (Oregon green 488) in green, for 3h. Intracellular and external/adhered *C. albicans* cells were distinguished based on fluorescence after co-staining with Calcofluor white in blue, which does not enter or stain macrophages. (C)

Phagocytic activity of macrophages at different times of interaction. (D) Environmental scanning electronic microscopy (ESEM) of macrophage and *C. albicans* co-culture after 3h of interaction

Figure 2. Gene Ontology (GO) analysis of the proteins considered differentially abundant after macrophage interaction with *C. albicans*. GO analysis of (A) molecular function, (B) biological process and (C) cellular component.

Figure 3. Predicted protein-protein interacting network using STRING (v10.0).

Some biological processes (RNA splicing, protein synthesis, proteolysis, endocytic traffic and apoptosis) are highlighted in the network, signaling some of the interacting proteins that are involved in each process. The network protein–protein interaction p -value was $5.76e^{-05}$.

Figure 4. Proteomic results validation in both conditions: Mφ (control) and Mφ+*C. albicans* (MOI 1 and 3 h of incubation). Quantification of: (A) MAP2K2, (B) PRDX5 and (C) ERK1/2 by Western blotting and (D) NDKA by selected reaction monitoring.

Figure 5. Caspase 3 activation and cytokine secretion measurement. Caspase activation was measured by Western blotting (A) and cytokine secretion measured using Enzyme-Linked ImmunoSorbent Assay (ELISA): (B) IL-1 β , (C) IL-12p40 and (D) TNF- α secretion in Mφ (control) and Mφ+*C. albicans* and after treatment with LPS (positive control).

Figure 6. Upstream-regulators predicted to be implicated in the response to *C. albicans* using Ingenuity® Pathway Analysis (IPA). The upstream regulators analysis is based on prior knowledge of expected effects between transcriptional regulators and their target genes stored in the IPA. (A) Bar chart of the upstream regulators that were predicted, including the activation z-score and p-value of each upstream regulator derived from IPA. Cellular validation of some of the upstream regulators was performed (B) IL-6 secretion by ELISA.


Figure 7. Expression levels of miRNAs in THP1 macrophages after interaction with *C. albicans* cells. Expression levels of (A) miR-21 and (B) mir-124 that were predicted by the IPA and (c) miR-146 and (D) miR-155 that were known to be activated after treatment with LPS and were used as controls.


Figure 8. Schematic overview of macrophage possible remodeling after interaction with *C. albicans*. The differentially abundant proteins, together with the cytokines, are color coded with red for more abundant and green for less abundant after macrophage interaction with *C. albicans*. The cytokines and the miR that do not present differences after interaction are depicted in grey. The text describes some of the processes suggested to be remodeled after interaction.

TABLES

Table 1. List of proteins differentially abundant 3 hours after macrophage-*C. albicans* interaction. Proteins are ordered by ratio average inside each category.

UniProt Code ^a	Entry Names	Gene names	Protein Names ^a	Ratio ^b	Standard Deviation ^b	Nr Replicates ^c
---------------------------	-------------	------------	----------------------------	--------------------	---------------------------------	----------------------------

 Proteins more abundant after macrophage interaction with <i>C. albicans</i>						
RNA processing						
O60812	HNRC1	HNRNPCL1	Heterogeneous nuclear ribonucleoprotein C-like 1	1.8	0.218	2
P14678	RSMB	SNRPB	Small nuclear ribonucleoprotein-associated proteins B and B'	1.5	0.045	3
Q99733	NP1L4	NAP1L4	Nucleosome assembly protein 1-like 4	1.4	0.169	2
Q01081	U2AF1	U2AF1	Splicing factor U2AF 35 kDa subunit	1.3	0.289	2
P09661	RU2A	SNRPA1	U2 small nuclear ribonucleoprotein A'	1.2	0.205	2
Q9NR30	DDX21	DDX21	Nucleolar RNA helicase 2	1.2	0.293	2
Structural components of ribosome						
P32969	RL9	RPL9	60S ribosomal protein L9	1.4	0.29	4
P62854	RS26	RPS26	40S ribosomal protein S26	1.3	0.166	2
P39023	RL3	RPL3	60S ribosomal protein L3	1.3	0.272	3
Oxidative stress						
P30044	PRDX5 ^d	PRDX5	Peroxiredoxin-5	1.3	0.171	2
Q6NUK1	SCMC1	SLC25A24	Calcium-binding mitochondrial carrier protein SCaMC-1	1.5	0.175	2
ATP production and transport						
O75964	ATP5L	ATP5L	ATP synthase subunit g	1.3	0.236	3
P05141	ADT2	SLC25A5	ADP/ATP translocase 2	1.2	0.227	4
Immune response and cell signalling						
P36507	MP2K2 ^d	MAP2K2	Dual specificity mitogen-activated protein kinase kinase 2	1.3	0.067	2
P43405	KSYK	SYK	Tyrosine-protein kinase SYK	1.2	0.187	2
Metabolism						
Q9NRN7	ADPPT	AASDHPPT	L-aminoadipate-semialdehyde dehydrogenase-phosphopantetheinyl transferase	1.4	0.075	3
Q8NBX0	SCPDL	SCCPDH	Saccharopine dehydrogenase-like oxidoreductase	1.3	0.066	2
Q9Y617	SERC	PSAT1	Phosphoserine aminotransferase	1.3	0.275	2

Others ^e						
B2RPK0	HGB1A	HMGB1P1	Putative high mobility group protein B1-like 1	1.3	0.251	3
P49589	SYCC	CARS	Cysteine--tRNA ligase	1.2	0.274	2
Q96QR8	PURB	PURB	Transcriptional activator protein Pur-beta	1.2	0.285	4
Q9Y6C9	MTCH2	MTCH2	Mitochondrial carrier homolog 2	1.2	0.237	4
 Proteins less abundant after macrophage interaction with <i>C. albicans</i>						
Proteolysis and peptide degradation						
Q9UHL4	DPP2	DPP7	Dipeptidyl peptidase 2	0.8	0.213	3
P14780	MMP9	MMP9	Matrix metalloproteinase-9	0.8	0.22	3
P28838	AMPL	LAP3	Cytosol aminopeptidase	0.8	0.237	4
Q96KP4	CNDP2	CNDP2	Cytosolic non-specific dipeptidase	0.8	0.076	2
P09960	LKHA4	LTA4H	Leukotriene A-4 hydrolase	0.8	0.284	4
P09622	DLDH	DLD	Dihydrolipoyl dehydrogenase	0.8	0.163	2
Transport						
Q8N5M9	JAGN1	JAGN1	Protein jagunal homolog 1	0.8	0.074	2
P51149	RAB7A	RAB7A	Ras-related protein Rab-7a	0.8	0.223	2
P84085	ARF5	ARF5	ADP-ribosylation factor 5	0.8	0.162	3
Proteasome components and protein fate						
P62333	PRS10	PSMC6	26S protease regulatory subunit 10B	0.9	0.104	3
P28065	PSB9	PSMB9	Proteasome subunit beta type-9	0.8	0.276	2
O94874	UFL1	UFL1	E3 UFM1-protein ligase 1	0.8	0.281	3
P51572	BAP31	BCAP31	B-cell receptor-associated protein 31	0.8	0.127	2
Immune response and cell signalling						
Q13188	STK3	STK3	Serine/threonine-protein kinase 3	0.8	0.061	2
Q9Y2U5	M3K2	MAP3K2	Mitogen-activated protein kinase kinase kinase 2	0.8	0.2	3
P36873	PP1G	PPP1CC	Serine/threonine-protein phosphatase PP1-gamma catalytic subunit	0.8	0.238	2
P09914	IFIT1	IFIT1	Interferon-induced protein with tetratricopeptide repeats 1	0.8	0.238	4
Q9Y6K5	OAS3	OAS3	2'-5'-oligoadenylate	0.8	0.233	4

synthase 3						
Cytoskeleton components/interactors and regulators						
Q15019	SEPT2	SEPT2	Septin-2	0.8	0.003	2
P46940	IQGA1	IQGAP1	Ras GTPase-activating-like protein IQGAP1	0.8	0.168	3
P20700	LMNB1	LMNB1	Lamin-B1	0.7	0.101	3
O43707	ACTN4	ACTN4	Alpha-actinin-4	0.6	0.096	3
Q68CZ2	TENS3	TNS3	Tensin-3	0.1	0.137	2
Ion transport and uptake						
Q13303	KCAB2	KCNAB2	Voltage-gated potassium channel subunit beta-2	0.8	0.093	2
P27105	STOM	STOM	Erythrocyte band 7 integral membrane protein	0.8	0.253	4
P02786	TFR1	TFRC	Transferrin receptor protein 1	0.5	0.115	2
RNA processing						
Q9Y3I0	RTCB	RTCB	tRNA-splicing ligase RtcB homolog	0.8	0.087	2
P29692	EF1D	EEF1D	Elongation factor 1-delta	0.8	0.057	2
Q96SB4	SRPK1	SRPK1	SRSF protein kinase 1	0.7	0.249	2
O43865	SAHH2	AHCYL1	Adenosylhomocysteinase 2	0.7	0.274	2
Nucleoside triphosphates synthesis						
P15531	NDKA ^d	NME1	Nucleoside diphosphate kinase A	0.8	0.228	2
P48047	ATPO	ATP5O	ATP synthase subunit O	0.7	0.098	3
Others^e						
Q9NSE4	SYIM	IARS2	Isoleucine--tRNA ligase	0.9	0.14	3
Q96IJ6	GMPPA	GMPPA	Mannose-1-phosphate guanylttransferase alpha	0.8	0.073	2
Q9NVJ2	ARL8B	ARL8B	ADP-ribosylation factor-like protein 8B	0.8	0.215	3
Q6S8J3	POTEE	POTEE	POTE ankyrin domain family member E	0.6	0.089	2
Q01432	AMPD3	AMPD3	AMP deaminase 3	0.5	0.278	4

^a Protein name and Uniprot Code according to Uniprot Knowledge base.

^b Average abundance ratio from macrophages + *C. albicans* versus control macrophages and respective inter-replicate standard deviation (cut-off in 0.3).

^c Proteins present in at least two biological replicates were considered and with a standard deviation lower than 30%

^d Proteins from this study that were validate by Western blot or SRM

^e In this category were included proteins with unknown or putative function and proteins that were not possible to include in the others categories

Table 2. List of ATP-binding Proteins quantified. Proteins are ordered by alphabetical and by protein family.

Protein Family	UniProt Code ^a	Entry name	Gene names	Protein Name
AAA ATPase family	P17980	PRS6A	PSMC3	26S protease regulatory subunit 6A
	P35998	PRS7	PSMC2	26S protease regulatory subunit 7
	P43686	PRS6B	PSMC4	26S protease regulatory subunit 6B
	P46459	NSF	NSF	Vesicle-fusing ATPase
	P55072	TERA	VCP	Transitional endoplasmic reticulum ATPase
	P62191	PRS4	PSMC1	26S protease regulatory subunit 4
	P62195	PRS8	PSMC5	26S protease regulatory subunit 8
	P62333	PRS10	PSMC6	26S protease regulatory subunit 10B ^b
ABC transporter superfamily	Q03518	TAP1	TAP1	Antigen peptide transporter 1
	P61221	ABCE1	ABCE1	ATP-binding cassette sub-family E member 1
Actin family	P60709	ACTB	ACTB	Actin. cytoplasmic 1
	P68032	ACTC	ACTC1	Actin. alpha cardiac muscle 1
	P61163	ACTZ	ACTR1A	Alpha-centractin
	P61160	ARP2	ACTR2	Actin-related protein 2
	P61158	ARP3	ACTR3	Actin-related protein 3
Adenylate kinase family	P00568	KAD1	AK1	Adenylate kinase isoenzyme 1
	P30085	KCY	CMPK1	UMP-CMP kinase
ATPase alpha/beta chains family	P06576	ATPB	ATP5F1B	ATP synthase subunit beta
	P25705	ATPA	ATP5F1A	ATP synthase subunit alpha
	P38606	VATA	ATP6V1A	V-type proton ATPase catalytic subunit A
Class-I aminoacyl-tRNA synthetase family	P23381	SYWC	WARS	Tryptophan-tRNA ligase
	P26640	SYVC	VARS	Valine-tRNA ligase
	P47897	SYQ	QARS	Glutamine-tRNA ligase
	P49589	SYCC	CARS	Cysteine-tRNA ligase ^c
	P54136	SYRC	RARS	Arginine-tRNA ligase
	P54577	SYYC	YARS	Tyrosine-tRNA ligase
	Q9NSE4	SYIM	IARS2	Isoleucine-tRNA ligase ^b

		Q9P2J5	SYLC	LARS	Leucine-tRNA ligase
		P07814	SYEP	EPRS	Bifunctional glutamate/proline-tRNA ligase
		O43776	SYNC	NARS	Asparagine-tRNA ligase
		P12081	SYHC	HARS	Histidine-tRNA ligase
		P26639	SYTC	TARS	Threonine-tRNA ligase
		P41250	GARS	GARS	Glycine-tRNA ligase
		P49588	SYAC	AARS	Alanine-tRNA ligase
		Q9Y285	SYFA	FARSA	Phenylalanine-tRNA ligase alpha subunit
		P14868	SYDC	DARS	Aspartate-tRNA ligase
		P49591	SYSC	SARS	Serine-tRNA ligase
ClpA/ClpB family		Q9H078	CLPB	CLPB	Caseinolytic peptidase B protein homolog
		O14656	TOR1A	TOR1A	Torsin-1A
DEAD box helicase family		Q9NR30	DDX21	DDX21	Nucleolar RNA helicase 2 °
		O00571	DDX3X	DDX3X	ATP-dependent RNA helicase DDX3X
		P17844	DDX5	DDX5	Probable ATP-dependent RNA helicase DDX5
		Q08211	DHX9	DHX9	ATP-dependent RNA helicase A
		O43143	DHX15	DHX15	Pre-mRNA-splicing factor ATP-dependent RNA helicase DHX15
		Q13838	DX39B	DDX39B	Spliceosome RNA helicase DDX39B
		P38919	IF4A3	EIF4A3	Eukaryotic initiation factor 4A-III
		P60842	IF4A1	EIF4A1	Eukaryotic initiation factor 4A-I
		Q14240	IF4A2	EIF4A2	Eukaryotic initiation factor 4A-II
Heat shock protein 70 family		P11021	BIP	HSPA5	78 kDa glucose-regulated protein
		P11142	HSP7C	HSPA8	Heat shock cognate 71 kDa protein
		P34932	HSP74	HSPA4	Heat shock 70 kDa protein 4
		P38646	GRP75	HSPA9	Stress-70 protein
		Q92598	HS105	HSPH1	Heat shock protein 105 kDa
		Q9Y4L1	HYOU1	HYOU1	Hypoxia up-regulated protein 1
Heat shock protein 90 family		P07900	HS90A	HSP90AA1	Heat shock protein HSP 90-alpha
		P08238	HS90B	HSP90AB1	Heat shock protein HSP 90-beta
		P14625	ENPL	HSP90B1	Endoplasmin
		Q12931	TRAP1	TRAP1	Heat shock protein 75 kDa
		Q58FF6	H90B4	HSP90AB4P	Putative heat shock protein HSP 90-beta 4
Phosphofructokinase type A (PFKA) family		P17858	PFKAL	PFKL	ATP-dependent 6-phosphofructokinase
		Q01813	PFKAP	PFKP	ATP-dependent 6-phosphofructokinase
Protein kinase superfamily	AGC Ser/Thr protein kinase family	P17612	KAPCA	PRKACA	cAMP-dependent protein kinase catalytic subunit alpha
		Q15418	KS6A1	RPS6KA1	Ribosomal protein S6 kinase

					alpha-1
	BUD32 family	Q96S44	PRPK	TP53RK	TP53-regulating kinase
	CMGC Ser/Thr protein kinase family	Q96SB4	SRPK1	SRPK1	SRSF protein kinase 1 ^b
		P49841	GSK3B	GSK3B	Glycogen synthase kinase-3 beta
		P28482	MK01	MAPK1	Mitogen-activated protein kinase 1
		Q16539	MK14	MAPK14	Mitogen-activated protein kinase 14
	Ser/Thr protein kinase family	P19784	CSK22	CSNK2A2	Casein kinase II subunit alpha'
		P68400	CSK21	CSNK2A1	Casein kinase II subunit alpha
		P19525	E2AK2	EIF2AK2	Interferon-induced, double-stranded RNA-activated protein kinase
	STE Ser/Thr protein kinase family	Q9Y2U5	M3K2	MAP3K2	Mitogen-activated protein kinase kinase kinase 2 ^b
		P36507	MP2K2	MAP2K2	Dual specificity mitogen-activated protein kinase kinase 2 ^c
		O94804	STK10	STK10	Serine/threonine-protein kinase 10
		O95747	OXS1	OXS1	Serine/threonine-protein kinase OSR1
		Q13043	STK4	STK4	Serine/threonine-protein kinase 4
		Q13177	PAK2	PAK2	Serine/threonine-protein kinase PAK 2
		Q13188	STK3	STK3	Serine/threonine-protein kinase 3 ^b
		Q9H2G2	SLK	SLK	STE20-like serine/threonine-protein kinase
		Q9H2K8	TAOK3	TAOK3	Serine/threonine-protein kinase TAO3
		Q9Y6E0	STK24	STK24	Serine/threonine-protein kinase 24
	TKL Ser/Thr protein kinase family	Q13418	ILK	ILK	Integrin-linked protein kinase
		Q9NWZ3	IRAK4	IRAK4	Interleukin-1 receptor-associated kinase 4
	Tyr protein kinase family. CSK subfamily	P41240	CSK	CSK	Tyrosine-protein kinase CSK
		P43405	KSYK	SYK	Tyrosine-protein kinase SYK ^c
	Ribose-phosphate pyrophosphokinase family	P11908	PRPS2	PRPS2	Ribose-phosphate pyrophosphokinase 2
		P60891	PRPS1	PRPS1	Ribose-phosphate pyrophosphokinase 1
	RtcB family	Q9Y310	RTCB	RTCB	tRNA-splicing ligase RtcB homolog ^b
		Q9Y230	RUVB2	RUVBL2	RuvB-like 2
		Q9Y265	RUVB1	RUVBL1	RuvB-like 1

Succinate/malate CoA ligase beta subunit family	Q9P2R7	SUCB1	SUCLA2	Succinate-CoA ligase
	Q96I99	SUCB2	SUCLG2	Succinate-CoA ligase
	P53396	ACLY	ACLY	ATP-citrate synthase
TCP-1 chaperonin family	P17987	TCPA	TCP1	T-complex protein 1 subunit alpha
	P40227	TCPZ	CCT6A	T-complex protein 1 subunit zeta
	P48643	TCPE	CCT5	T-complex protein 1 subunit epsilon
	P49368	TCPG	CCT3	T-complex protein 1 subunit gamma
	P50990	TCPQ	CCT8	T-complex protein 1 subunit theta
	P50991	TCPD	CCT4	T-complex protein 1 subunit delta
	P78371	TCPB	CCT2	T-complex protein 1 subunit beta
	Q99832	TCPH	CCT7	T-complex protein 1 subunit eta
Ubiquitin-activating E1 family	A0AVT1	UBA6	UBA6	Ubiquitin-like modifier-activating enzyme 6
	P22314	UBA1	UBA1	Ubiquitin-like modifier-activating enzyme 1
	Q9UBT2	SAE2	UBA2	SUMO-activating enzyme subunit 2
	Q9GZZ9	UBA5	UBA5	Ubiquitin-like modifier-activating enzyme 5
	P61088	UBE2N	UBE2N	Ubiquitin-conjugating enzyme E2 N
Proteins without Protein Family assigned	P05165	PCCA	PCCA	Propionyl-CoA carboxylase alpha chain
	P48426	PI42A	PIP4K2A	Phosphatidylinositol 5-phosphate 4-kinase type-2 alpha
	P49915	GUAA	GMPS	GMP synthase
	Q02790	FKBP4	FKBP4	Peptidyl-prolyl cis-trans isomerase FKBP4
	Q12905	ILF2	ILF2	Interleukin enhancer-binding factor 2
	Q14166	TTL12	TTLL12	Tubulin--tyrosine ligase-like protein 12
	Q9UHD1	CHRD1	CHORDC1	Cysteine and histidine-rich domain-containing protein 1
Other ATP-binding Proteins	Q9Y6K5	OAS3	OAS3	2'-5'-oligoadenylate synthase 3 ^b
	P00966	ASSY	ASS1	Argininosuccinate synthase
	O43681	ASNA	ASNA1	ATPase ASNA1
	O60488	ACSL4	ACSL4	Long-chain-fatty-acid--CoA ligase 4
	P16615	AT2A2	ATP2A2	Sarcoplasmic/endoplasmic reticulum calcium ATPase 2
	P10809	CH60	HSPD1	60 kDa heat shock protein
	P17812	PYRG1	CTPS1	CTP synthase 1
	Q13057	COASY	COASY	Bifunctional coenzyme A synthase
	P22102	PUR2	GART	Trifunctional purine biosynthetic protein adenosine-3
	P00367	DHE3	GLUD1	Glutamate dehydrogenase 1
	P54886	P5CS	ALDH18A1	Delta-1-pyrroline-5-carboxylate synthase
	P19367	HXK1	HK1	Hexokinase-1

	P12956	XRCC6	XRCC6	X-ray repair cross-complementing protein 6
	P13010	XRCC5	XRCC5	X-ray repair cross-complementing protein 5
	P15531	NDKA	NME1	Nucleoside diphosphate kinase A _b
	P36776	LONM	LONP1	Lon protease homolog
	Q9NSD9	SYFB	FARSB	Phenylalanine--tRNA ligase beta subunit
	P00558	PGK1	PGK1	Phosphoglycerate kinase 1
	P14618	KPYM	PKM	Pyruvate kinase PKM
	P22234	PUR6	PAICS	Multifunctional protein ADE2
	P11586	C1TC	MTHFD1	C-1-tetrahydrofolate synthase
	O43615	TIM44	TIMM44	Mitochondrial import inner membrane translocase subunit TIM44
	Q12965	MYO1E	MYO1E	Unconventional myosin-le
	Q9NTK5	OLA1	OLA1	Obg-like ATPase 1

^a Uniprot Code according to Uniprot Knowledge base. Proteins only with a standard deviation lower than 30% and quantified in at least 2 biological replicates.

^b Proteins annotated as ATP-binding proteins in Uniprot database that were found in this study to be less abundant during macrophage interaction with *C. albicans*.

^c Proteins annotated as ATP-binding proteins in Uniprot database that were found in this study to be more abundant during macrophage interaction with *C. albicans*.

Table 3. List of phosphopeptides differentially abundant after 3 hours of macrophage - *C. albicans* interaction.

UniProt Code ^a	Gene names	Protein names ^a	Phosphopeptide	Phosphosite ^b	Ratio ^c	SD ^c
Q13131	PRKAA1	5'-AMP-activated protein kinase catalytic subunit alpha-1	SGSVSNYR	ambiguous	1.58	0.22
Q9NWW5	CLN6	Ceroid-lipofuscinosis neuronal protein 6	HGs*VSADEAAR ^d	Ser31	1.40	0.29
Q9BTU6	PI4K2A	Phosphatidylinositol 4-kinase type 2-alpha	SSSESYTQSFQSR	ambiguous	0.70	0.22
P12931	SRC	Proto-oncogene tyrosine-protein kinase Src	LIEDNEy*TAR	Tyr419	0.69	0.22
Q05655	PRKCD	Protein kinase C delta type	SDSASSEPVGIYQGFEK	ambiguous	0.57	0.06

^a Protein name and Uniprot Code according to Uniprot Knowledge base.

^b Phosphosites were considered ambiguous in case PhosphoRS algorithm assigned a localization probability lower than 75% or if it was assigned in distinct sites in different biological replicates.

^c Average abundance ratio from macrophages + *C. albicans* versus control macrophages and respective inter-replicate standard deviation (cut-off in 0.3). Only phosphopeptides with a standard deviation lower than 30% and quantified in at least 2 biological replicates.

^d Asterisk indicates the phosphorylation site and the corresponding aminoacid is in lower case.

ASSOCIATED CONTENT

Supporting Information

Figure S1. Schematic workflow of the experiment performed.

Figure S2. Venn diagram showing the identified proteins in each replicate.

Figure S3. GO analysis of proteins quantified after ATP-binding proteins enrichment.

Figure S4. Histogram showing log₂-transformed mean of THP-1 macrophage protein abundance ratios upon *C. albicans* interaction.

Figure S5. Histogram showing log₂-transformed mean of THP-1 macrophage phosphopeptide abundance ratios upon *C. albicans* interaction.

Figure S6. Mass spectra of the differentially abundant phosphopeptides.

Figure S7. Quantification of P-ERK1/2 by Western blotting.

Figure S8. Calibration curve of the peptide FMQASEDLLK from NDKA protein.

Table S1. List of proteins identified in THP-1 macrophages after interaction with *C. albicans*.

Table S2. List of proteins quantified in THP-1 macrophages after interaction with *C. albicans*.

Table S3. GO analysis of the proteins from our dataset annotated in Uniprot as “ATP binding protein”.

Table S4. List of phosphopeptides quantified in THP-1 macrophages after interaction with *C. albicans*.

Table S5. Calibration curve of the heavy peptide and endogenous peptide quantification by SRM.

AUTHOR INFORMATION

Corresponding Author

* Lucia Monteoliva: e-mail: luciamon@ucm.es; phone: +34913941748; Fax: +34913941745

Present Addresses

† Singapore Immunology Network (SIgN), A*STAR; 8A Biomedical Grove, Level 4, Immunos (Biopolis), Singapore, 138648, Singapore

Author Contributions

The manuscript was written through contributions of all authors. All authors have given approval to the final version of the manuscript.

Notes

The authors declare no competing financial interest.

ACKNOWLEDGEMENTS

This study was supported by the Marie Curie Initial Training Network (FP7-PEOPLE-2013-ITN ImResFun), the project BIO2015-65147-R from Spanish Ministry of Economy and Competitiveness (MINECO), InGEMICS-CM B2017/BMD-3691 from

the Comunidad de Madrid, Spanish Network for the Research in Infectious Diseases (REIPI RD16/0016/0011) and PRB3 (PT17/0019/0012) from the ISCIII. InGEMICS-CM, REIPI and PRB3 are co-financed by European Development Regional Fund ERDF “A way to achieve Europe”. These results are lined up with the Human Infectious Diseases HPP initiative from the Human Proteome Project (HID-HPP). The ESEM was performed in Museo Nacional de Ciencias Naturales. The proteomics analyses were performed in Centro de Investigaciones Biológicas (CIB) and Proteomics Facility of Complutense University of Madrid (UCM), both members of ProteoRed-ISCIII network. The miRNA analysis was carried out in Genomics Facility of Complutense University of Madrid. The authors would like to thank Leif Schauser and Nitesh Kumar Singh from QIAGEN (Aarhus) IMRESFUN consortium partners for their help in IPA analysis.

ABBREVIATIONS

CLRs - c-type lectin receptors, DMEM - Dulbecco's modified eagle's medium, ELISA - enzyme-linked immunosorbent assay, ESEM - environmental scanning electron microscopy, FBS – fetal bovine serum, GO - gene ontology, IFNs – interferons, IL – interleukin, IPA - Ingenuity Pathway Analysis, LDH – lactate dehydrogenase, LPS – lipopolysaccharide, MOI - multiplicity of infection, NODs - nod-like receptors, PBS – phosphate buffer saline, PMA - phorbol 12-myristate 13-acetate, PRRs - pattern recognition receptors, RIPA - radio immunoprecipitation assay buffer, ROS - reactive oxygen species, RT-PCR – real time polymerase chain reaction, SD - standard deviation, STE - ser/thr protein kinase family, TLRs – toll-like receptors, TR - transcription regulator, YPD – Yeast peptone dextrose

REFERENCES

1. Erwig, L. P.;Gow, N. A. Interactions of fungal pathogens with phagocytes. *Nature reviews. Microbiology* **2016**, *14* (3), 163-76.
2. Pfaller, M. A.;Castanheira, M. Nosocomial Candidiasis: Antifungal Stewardship and the Importance of Rapid Diagnosis. *Medical mycology* **2016**, *54* (1), 1-22.
3. Nieto, M. C.; Telleria, O.;Cisterna, R. Sentinel surveillance of invasive candidiasis in Spain: epidemiology and antifungal susceptibility. *Diagnostic microbiology and infectious disease* **2015**, *81* (1), 34-40.
4. Bourgeois, C.; Majer, O.; Frohner, I. E.; Tierney, L.;Kuchler, K. Fungal attacks on mammalian hosts: pathogen elimination requires sensing and tasting. *Current opinion in microbiology* **2010**, *13* (4), 401-8.
5. West, A. P.; Koblansky, A. A.;Ghosh, S. Recognition and signaling by toll-like receptors. *Annual review of cell and developmental biology* **2006**, *22*, 409-37.
6. Reales-Calderon, J. A.; Martinez-Solano, L.; Martinez-Gomariz, M.; Nombela, C.; Molero, G.;Gil, C. Sub-proteomic study on macrophage response to *Candida albicans* unravels new proteins involved in the host defense against the fungus. *Journal of proteomics* **2012**, *75* (15), 4734-46.
7. Reales-Calderon, J. A.; Sylvester, M.; Strijbis, K.; Jensen, O. N.; Nombela, C.; Molero, G.;Gil, C. *Candida albicans* induces pro-inflammatory and anti-apoptotic signals in macrophages as revealed by quantitative proteomics and phosphoproteomics. *Journal of proteomics* **2013**, *91*, 106-35.
8. Reales-Calderon, J. A.; Aguilera-Montilla, N.; Corbi, A. L.; Molero, G.;Gil, C. Proteomic characterization of human proinflammatory M1 and anti-inflammatory M2 macrophages and their response to *Candida albicans*. *Proteomics* **2014**, *14* (12), 1503-18.

9. Shin, Y. K.; Kim, K. Y.; Paik, Y. K. Alterations of protein expression in macrophages in response to *Candida albicans* infection. *Mol Cells* **2005**, *20* (2), 271-9.
10. Kitahara, N.; Morisaka, H.; Aoki, W.; Takeda, Y.; Shibasaki, S.; Kuroda, K.; Ueda, M. Description of the interaction between *Candida albicans* and macrophages by mixed and quantitative proteome analysis without isolation. *Amb Express* **2015**, *5* (41), 1-12.
11. Xiao, Y.; Wang, Y. Global discovery of protein kinases and other nucleotide-binding proteins by mass spectrometry. *Mass spectrometry reviews* **2014**, *35*, 601-619.
12. Guo, L.; Xiao, Y.; Fan, M.; Li, J. J.; Wang, Y. Profiling Global Kinome Signatures of the Radioresistant MCF-7/C6 Breast Cancer Cells Using MRM-based Targeted Proteomics. *Journal of proteome research* **2014**.
13. Wolfe, L. M.; Veeraraghavan, U.; Idicula-Thomas, S.; Schurer, S.; Wennerberg, K.; Reynolds, R.; Besra, G. S.; Dobos, K. M. A chemical proteomics approach to profiling the ATP-binding proteome of Mycobacterium tuberculosis. *Molecular & cellular proteomics : MCP* **2013**, *12* (6), 1644-60.
14. Villamor, J. G.; Kaschani, F.; Colby, T.; Oeljeklaus, J.; Zhao, D.; Kaiser, M.; Patricelli, M. P.; van der Hoorn, R. A. Profiling protein kinases and other ATP binding proteins in Arabidopsis using Acyl-ATP probes. *Molecular & cellular proteomics : MCP* **2013**, *12* (9), 2481-96.
15. Adachi, J.; Kishida, M.; Watanabe, S.; Hashimoto, Y.; Fukamizu, K.; Tomonaga, T. Proteome-Wide Discovery of Unknown ATP-Binding Proteins and Kinase Inhibitor Target Proteins Using an ATP Probe (vol 13, pg 5461, 2014). *Journal of proteome research* **2015**, *14* (2), 1333-1333.
16. Xiao, Y.; Guo, L.; Wang, Y. Isotope-coded ATP probe for quantitative affinity profiling of ATP-binding proteins. *Analytical chemistry* **2013**, *85* (15), 7478-86.

17. Graves, P. R.; Kwiek, J. J.; Fadden, P.; Ray, R.; Hardeman, K.; Coley, A. M.; Foley, M.; Haystead, T. A. Discovery of novel targets of quinoline drugs in the human purine binding proteome. *Molecular pharmacology* **2002**, *62* (6), 1364-72.
18. Daub, H.; Olsen, J. V.; Bairlein, M.; Gnad, F.; Oppermann, F. S.; Korner, R.; Greff, Z.; Keri, G.; Stemmann, O.; Mann, M. Kinase-selective enrichment enables quantitative phosphoproteomics of the kinome across the cell cycle. *Molecular cell* **2008**, *31* (3), 438-48.
19. Hanoulle, X.; Van Damme, J.; Staes, A.; Martens, L.; Goethals, M.; Vandekerckhove, J.; Gevaert, K. A new functional, chemical proteomics technology to identify purine nucleotide binding sites in complex proteomes. *Journal of proteome research* **2006**, *5* (12), 3438-45.
20. Duncan, J. S.; Whittle, M. C.; Nakamura, K.; Abell, A. N.; Midland, A. A.; Zawistowski, J. S.; Johnson, N. L.; Granger, D. A.; Jordan, N. V.; Darr, D. B.; Usary, J.; Kuan, P. F.; Smalley, D. M.; Major, B.; He, X.; Hoadley, K. A.; Zhou, B.; Sharpless, N. E.; Perou, C. M.; Kim, W. Y.; Gomez, S. M.; Chen, X.; Jin, J.; Frye, S. V.; Earp, H. S.; Graves, L. M.; Johnson, G. L. Dynamic reprogramming of the kinome in response to targeted MEK inhibition in triple-negative breast cancer. *Cell* **2012**, *149* (2), 307-21.
21. Patricelli, M. P.; Szardenings, A. K.; Liyanage, M.; Nomanbhoy, T. K.; Wu, M.; Weissig, H.; Aban, A.; Chun, D.; Tanner, S.; Kozarich, J. W. Functional Interrogation of the Kinome Using Nucleotide Acyl Phosphates. *The Biochemical journal* **2007**, *46*, 350-358.
22. Ong, S. E.; Mann, M. A practical recipe for stable isotope labeling by amino acids in cell culture (SILAC). *Nature protocols* **2006**, *1* (6), 2650-60.

23. Blagoev, B.; Kratchmarova, I.; Ong, S. E.; Nielsen, M.; Foster, L. J.; Mann, M. A proteomics strategy to elucidate functional protein-protein interactions applied to EGF signaling. *Nature biotechnology* **2003**, *21* (3), 315-8.
24. Huang, J.; Wang, F.; Ye, M.; Zou, H. Enrichment and separation techniques for large-scale proteomics analysis of the protein post-translational modifications. *Journal of chromatography. A* **2014**, *1372C*, 1-17.
25. Reales-Calderon, J. A.; Vaz, C.; Monteoliva, L.; Molero, G.; Gil, C. *Candida albicans* Modifies the Protein Composition and Size Distribution of THP1 macrophages-derived Extracellular Vesicles. *Journal of proteome research* **2016**, *16* (1), 87-105.
26. Fernandez-Arenas, E.; Cabezon, V.; Bermejo, C.; Arroyo, J.; Nombela, C.; Diez-Orejas, R.; Gil, C. Integrated proteomics and genomics strategies bring new insight into *Candida albicans* response upon macrophage interaction. *Molecular & cellular proteomics : MCP* **2007**, *6* (3), 460-78.
27. Bonzon-Kulichenko, E.; Perez-Hernandez, D.; Nunez, E.; Martinez-Acedo, P.; Navarro, P.; Trevisan-Herraz, M.; Ramos Mdel, C.; Sierra, S.; Martinez-Martinez, S.; Ruiz-Meana, M.; Miro-Casas, E.; Garcia-Dorado, D.; Redondo, J. M.; Burgos, J. S.; Vazquez, J. A robust method for quantitative high-throughput analysis of proteomes by 18O labeling. *Molecular & cellular proteomics : MCP* **2011**, *10* (1), M110 003335.
28. Shevchenko, A.; Tomas, H.; Havlis, J.; Olsen, J. V.; Mann, M. In-gel digestion for mass spectrometric characterization of proteins and proteomes. *Nature protocols* **2006**, *1* (6), 2856-60.
29. Picotti, P.; Aebersold, R. Selected reaction monitoring-based proteomics: workflows, potential, pitfalls and future directions. *Nature methods* **2012**, *9* (6), 555-66.

30. Carmona-Saez, P.; Chagoyen, M.; Tirado, F.; Carazo, J. M.; Pascual-Montano, A. GENECODIS: a web-based tool for finding significant concurrent annotations in gene lists. *Genome Biol* **2007**, *8* (1), R3.
31. Nogales-Cadenas, R.; Carmona-Saez, P.; Vazquez, M.; Vicente, C.; Yang, X.; Tirado, F.; Carazo, J. M.; Pascual-Montano, A. GeneCodis: interpreting gene lists through enrichment analysis and integration of diverse biological information. *Nucleic acids research* **2009**, *37* (Web Server issue), W317-22.
32. Tabas-Madrid, D.; Nogales-Cadenas, R.; Pascual-Montano, A. GeneCodis3: a non-redundant and modular enrichment analysis tool for functional genomics. *Nucleic acids research* **2012**, *40* (Web Server issue), W478-83.
33. Szklarczyk, D.; Morris, J. H.; Cook, H.; Kuhn, M.; Wyder, S.; Simonovic, M.; Santos, A.; Doncheva, N. T.; Roth, A.; Bork, P.; Jensen, L. J.; von Mering, C. The STRING database in 2017: quality-controlled protein-protein association networks, made broadly accessible. *Nucleic acids research* **2017**, *45* (D1), D362-D368.
34. Livak, K. J.; Schmittgen, T. D. Analysis of relative gene expression data using real-time quantitative PCR and the 2(-Delta Delta C(T)) Method. *Methods* **2001**, *25* (4), 402-8.
35. Fernandez-Arenas, E.; Bleck, C. K.; Nombela, C.; Gil, C.; Griffiths, G.; Diez-Orejas, R. *Candida albicans* actively modulates intracellular membrane trafficking in mouse macrophage phagosomes. *Cellular microbiology* **2009**, *11* (4), 560-89.
36. Traba, J.; Del Arco, A.; Duchon, M. R.; Szabadkai, G.; Satrustegui, J. SCaMC-1 promotes cancer cell survival by desensitizing mitochondrial permeability transition via ATP/ADP-mediated matrix Ca(2+) buffering. *Cell Death Differ* **2012**, *19* (4), 650-60.
37. Shiota, M.; Izumi, H.; Miyamoto, N.; Onitsuka, T.; Kashiwagi, E.; Kidani, A.; Hirano, G.; Takahashi, M.; Ono, M.; Kuwano, M.; Naito, S.; Sasaguri, Y.; Kohno, K.

Ets regulates peroxiredoxin1 and 5 expressions through their interaction with the high-mobility group protein B1. *Cancer Sci* **2008**, *99* (10), 1950-9.

38. Wang, Q.; Sawyer, I. A.; Sung, M. H.; Sturgill, D.; Shevtsov, S. P.; Pegoraro, G.; Hakim, O.; Baek, S.; Hager, G. L.; Dundr, M. Cajal bodies are linked to genome conformation. *Nat Commun* **2016**, *7*, 10966.

39. Arthur, J. S.; Ley, S. C. Mitogen-activated protein kinases in innate immunity. *Nature reviews. Immunology* **2013**, *13* (9), 679-92.

40. Yuan, J.; Murrell, G. A.; Trickett, A.; Landtmeters, M.; Knoops, B.; Wang, M. X. Overexpression of antioxidant enzyme peroxiredoxin 5 protects human tendon cells against apoptosis and loss of cellular function during oxidative stress. *Biochim Biophys Acta* **2004**, *1693* (1), 37-45.

41. Jang, J. Y.; Choi, Y.; Jeon, Y. K.; Kim, C. W. Suppression of adenine nucleotide translocase-2 by vector-based siRNA in human breast cancer cells induces apoptosis and inhibits tumor growth in vitro and in vivo. *Breast Cancer Res* **2008**, *10* (1), R11.

42. Lee, J. H.; Choi, Y. J.; Park, S. H.; Nam, M. J. Potential role of nucleoside diphosphate kinase in myricetin-induced selective apoptosis in colon cancer HCT-15 cells. *Food Chem Toxicol* **2018**, *116* (Pt B), 315-322.

43. Liu, Q. Y.; Lei, J. X.; LeBlanc, J.; Sodja, C.; Ly, D.; Charlebois, C.; Walker, P. R.; Yamada, T.; Hirohashi, S.; Sikorska, M. Regulation of DNaseY activity by actinin- α 4 during apoptosis. *Cell Death Differ* **2004**, *11* (6), 645-54.

44. Lee, K. K.; Ohyama, T.; Yajima, N.; Tsubuki, S.; Yonehara, S. MST, a physiological caspase substrate, highly sensitizes apoptosis both upstream and downstream of caspase activation. *The Journal of biological chemistry* **2001**, *276* (22), 19276-85.

45. Shalini, S.; Dorstyn, L.; Dawar, S.; Kumar, S. Old, new and emerging functions of caspases. *Cell Death Differ* **2015**, *22* (4), 526-39.
46. Uwamahoro, N.; Verma-Gaur, J.; Shen, H. H.; Qu, Y.; Lewis, R.; Lu, J.; Bambery, K.; Masters, S. L.; Vince, J. E.; Naderer, T.; Traven, A. The pathogen *Candida albicans* hijacks pyroptosis for escape from macrophages. *MBio* **2014**, *5* (2), e00003-14.
47. Bergsbaken, T.; Fink, S. L.; Cookson, B. T. Pyroptosis: host cell death and inflammation. *Nature reviews. Microbiology* **2009**, *7* (2), 99-109.
48. Tsitsiou, E.; Lindsay, M. A. microRNAs and the immune response. *Curr Opin Pharmacol* **2009**, *9* (4), 514-20.
49. Taganov, K. D.; Boldin, M. P.; Chang, K. J.; Baltimore, D. NF-kappaB-dependent induction of microRNA miR-146, an inhibitor targeted to signaling proteins of innate immune responses. *Proceedings of the National Academy of Sciences of the United States of America* **2006**, *103* (33), 12481-6.
50. Agostinho, D. P.; de Oliveira, M. A.; Tavares, A. H.; Derengowski, L.; Stolz, V.; Guilhelmelli, F.; Mortari, M. R.; Kuchler, K.; Silva-Pereira, I. Dectin-1 is required for miR155 upregulation in murine macrophages in response to *Candida albicans*. *Virulence* **2016**, 1-12.
51. Monk, C. E.; Hutvagner, G.; Arthur, J. S. Regulation of miRNA transcription in macrophages in response to *Candida albicans*. *PloS one* **2010**, *5* (10), e13669.
52. Pappas, P. G.; Lionakis, M. S.; Arendrup, M. C.; Ostrosky-Zeichner, L.; Kullberg, B. J. Invasive candidiasis. *Nat Rev Dis Primers* **2018**, *4*, 18026.
53. Carpino, N.; Naseem, S.; Frank, D. M.; Konopka, J. B. Modulating Host Signaling Pathways to Promote Resistance to Infection by *Candida albicans*. *Frontiers in cellular and infection microbiology* **2017**, *7*, 481.

54. Zwolanek, F.; Riedelberger, M.; Stolz, V.; Jenull, S.; Istel, F.; Koprulu, A. D.; Ellmeier, W.; Kuchler, K. The non-receptor tyrosine kinase Tec controls assembly and activity of the noncanonical caspase-8 inflammasome. *PLoS pathogens* **2014**, *10* (12), e1004525.
55. Singh, A. K.; Pandey, R. K.; Siqueira-Neto, J. L.; Kwon, Y. J.; Freitas, L. H.; Shaha, C.; Madhubala, R. Proteomic-Based Approach To Gain Insight into Reprogramming of THP-1 Cells Exposed to *Leishmania donovani* over an Early Temporal Window. *Infection and immunity* **2015**, *83* (5), 1853-1868.
56. Duan, Z.; Chen, X.; Du, L.; Liu, C.; Zeng, R.; Chen, Q.; Li, M. Inflammation Induced by *Candida parapsilosis* in THP-1 Cells and Human Peripheral Blood Mononuclear Cells (PBMCs). *Mycopathologia* **2017**, *182* (11-12), 1015-1023.
57. Kaewseekhao, B.; Naranbhai, V.; Roytrakul, S.; Namwat, W.; Paemanee, A.; Lulitanond, V.; Chaiprasert, A.; Faksri, K. Comparative Proteomics of Activated THP-1 Cells Infected with *Mycobacterium tuberculosis* Identifies Putative Clearance Biomarkers for Tuberculosis Treatment. *PloS one* **2015**, *10* (7), e0134168.
58. Barker, K. S.; Liu, T.; Rogers, P. D. Coculture of THP-1 human mononuclear cells with *Candida albicans* results in pronounced changes in host gene expression. *The Journal of infectious diseases* **2005**, *192* (5), 901-12.
59. Chanput, W.; Mes, J. J.; Wichers, H. J. THP-1 cell line: An in vitro cell model for immune modulation approach. *International immunopharmacology* **2014**, *23* (1), 37-45.
60. Lemeer, S.; Zorgiebel, C.; Ruprecht, B.; Kohl, K.; Kuster, B. Comparing immobilized kinase inhibitors and covalent ATP probes for proteomic profiling of kinase expression and drug selectivity. *Journal of proteome research* **2013**, *12* (4), 1723-31.

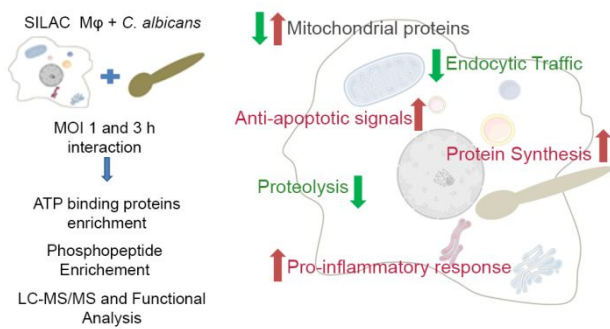
61. Oppermann, F. S.; Gnad, F.; Olsen, J. V.; Hornberger, R.; Greff, Z.; Keri, G.; Mann, M.; Daub, H. Large-scale proteomics analysis of the human kinome. *Molecular & cellular proteomics : MCP* **2009**, 8 (7), 1751-64.
62. Sun, G.; Yao, F.; Tian, Z.; Ma, T.; Yang, Z. A first CLN6 variant case of late infantile neuronal ceroid lipofuscinosis caused by a homozygous mutation in a boy from China: a case report. *BMC Med Genet* **2018**, 19 (1), 177.
63. Bae, H. B.; Zmijewski, J. W.; Deshane, J. S.; Tadie, J. M.; Chaplin, D. D.; Takashima, S.; Abraham, E. AMP-activated protein kinase enhances the phagocytic ability of macrophages and neutrophils. *FASEB J* **2011**, 25 (12), 4358-68.
64. Lizcano, J. M.; Goransson, O.; Toth, R.; Deak, M.; Morrice, N. A.; Boudeau, J.; Hawley, S. A.; Udd, L.; Makela, T. P.; Hardie, D. G.; Alessi, D. R. LKB1 is a master kinase that activates 13 kinases of the AMPK subfamily, including MARK/PAR-1. *Embo Journal* **2004**, 23 (4), 833-843.
65. Pandey, A.; Ding, S. L.; Qin, Q. M.; Gupta, R.; Gomez, G.; Lin, F.; Feng, X.; Fachini da Costa, L.; Chaki, S. P.; Katepalli, M.; Case, E. D.; van Schaik, E. J.; Sidiq, T.; Khalaf, O.; Arenas, A.; Kobayashi, K. S.; Samuel, J. E.; Rivera, G. M.; Alaniz, R. C.; Sze, S. H.; Qian, X.; Brown, W. J.; Rice-Ficht, A.; Russell, W. K.; Ficht, T. A.; de Figueiredo, P. Global Reprogramming of Host Kinase Signaling in Response to Fungal Infection. *Cell host & microbe* **2017**, 21 (5), 637-649 e6.
66. Hawley, S. A.; Ross, F. A.; Gowans, G. J.; Tibarewal, P.; Leslie, N. R.; Hardie, D. G. Phosphorylation by Akt within the ST loop of AMPK- α 1 down-regulates its activation in tumour cells. *Biochemical Journal* **2014**, 459, 275-287.
67. Netea, M. G.; Joosten, L. A.; van der Meer, J. W.; Kullberg, B. J.; van de Veerdonk, F. L. Immune defence against *Candida* fungal infections. *Nature reviews. Immunology* **2015**, 15 (10), 630-42.

68. Zhang, Y.; Tu, Y.; Zhao, J.; Chen, K.; Wu, C. Reversion-induced LIM interaction with Src reveals a novel Src inactivation cycle. *J Cell Biol* **2009**, *184* (6), 785-92.
69. Byeon, S. E.; Yi, Y. S.; Oh, J.; Yoo, B. C.; Hong, S.; Cho, J. Y. The Role of Src Kinase in Macrophage-Mediated Inflammatory Responses. *Mediators of inflammation* **2012**, *2012*, 1-18.
70. Minogue, S.; Waugh, M. G.; De Matteis, M. A.; Stephens, D. J.; Berditchevski, F.; Hsuan, J. J. Phosphatidylinositol 4-kinase is required for endosomal trafficking and degradation of the EGF receptor. *Journal of Cell Science* **2006**, *119* (3), 571-580.
71. Via, L. E.; Deretic, D.; Ulmer, R. J.; Hibler, N. S.; Huber, L. A.; Deretic, V. Arrest of mycobacterial phagosome maturation is caused by a block in vesicle fusion between stages controlled by rab5 and rab7. *Journal of Biological Chemistry* **1997**, *272* (20), 13326-13331.
72. Vergne, I.; Fratti, R. A.; Hill, P. J.; Chua, J.; Belisle, J.; Deretic, V. *Mycobacterium tuberculosis* phagosome maturation arrest: mycobacterial phosphatidylinositol analog phosphatidylinositol mannoside stimulates early endosomal fusion. *Mol Biol Cell* **2004**, *15* (2), 751-60.
73. Rothenberger, S.; Iacopetta, B. J.; Kuhn, L. C. Endocytosis of the transferrin receptor requires the cytoplasmic domain but not its phosphorylation site. *Cell* **1987**, *49* (3), 423-31.
74. Forman, H. J.; Torres, M. Redox signaling in macrophages. *Mol Aspects Med* **2001**, *22* (4-5), 189-216.
75. Choi, H. I.; Chung, K. J.; Yang, H. Y.; Ren, L.; Sohn, S.; Kim, P. R.; Kook, M. S.; Choy, H. E.; Lee, T. H. Peroxiredoxin V selectively regulates IL-6 production by modulating the Jak2-Stat5 pathway. *Free Radic Biol Med* **2013**, *65*, 270-9.

76. Shui, W.; Gilmore, S. A.; Sheu, L.; Liu, J.; Keasling, J. D.; Bertozzi, C. R. Quantitative proteomic profiling of host-pathogen interactions: the macrophage response to *Mycobacterium tuberculosis* lipids. *Journal of proteome research* **2009**, *8* (1), 282-9.
77. Liu, P. S.; Ho, P. C. Mitochondria: A master regulator in macrophage and T cell immunity. *Mitochondrion* **2017**, *41* (2018), 45-50.
78. Tazi, J.; Bakkour, N.; Stamm, S. Alternative splicing and disease. *Biochim Biophys Acta* **2009**, *1792* (1), 14-26.
79. Geuens, T.; Bouhy, D.; Timmerman, V. The hnRNP family: insights into their role in health and disease. *Hum Genet* **2016**, *135* (8), 851-867.
80. Choi, Y. D.; Grabowski, P. J.; Sharp, P. A.; Dreyfuss, G. Heterogeneous nuclear ribonucleoproteins: role in RNA splicing. *Science* **1986**, *231* (4745), 1534-9.
81. McIlwain, D. R.; Berger, T.; Mak, T. W. Caspase functions in cell death and disease. *Cold Spring Harbor perspectives in biology* **2013**, *5* (4), a008656.
82. Vylkova, S.; Lorenz, M. C. Phagosomal Neutralization by the Fungal Pathogen *Candida albicans* Induces Macrophage Pyroptosis. *Infection and immunity* **2017**, *85* (2).
83. O'Meara, T. R.; Veri, A. O.; Ketela, T.; Jiang, B.; Roemer, T.; Cowen, L. E. Global analysis of fungal morphology exposes mechanisms of host cell escape. *Nat Commun* **2015**, *6*, 6741.
84. Wellington, M.; Koselny, K.; Krysan, D. J. *Candida albicans* morphogenesis is not required for macrophage interleukin 1beta production. *MBio* **2012**, *4* (1), e00433-12.
85. Netea, M. G.; Brown, G. D.; Kullberg, B. J.; Gow, N. A. An integrated model of the recognition of *Candida albicans* by the innate immune system. *Nature reviews. Microbiology* **2008**, *6* (1), 67-78.

- 1
2
3 86. Kramer, A.; Green, J.; Pollard, J., Jr.;Tugendreich, S. Causal analysis
4 approaches in Ingenuity Pathway Analysis. *Bioinformatics* **2014**, *30* (4), 523-30.
5
6
7
8 87. Estrada-Mata, E.; Navarro-Arias, M. J.; Perez-Garcia, L. A.; Mellado-Mojica,
9 E.; Lopez, M. G.; Csonka, K.; Gacser, A.;Mora-Montes, H. M. Members of the
10 *Candida parapsilosis* Complex and *Candida albicans* are Differentially Recognized by
11 Human Peripheral Blood Mononuclear Cells. *Frontiers in microbiology* **2015**, *6*, 1527.
12
13
14
15
16
17 88. Martinez-Solano, L.; Reales-Calderon, J. A.; Nombela, C.; Molero, G.;Gil, C.
18 Proteomics of RAW 264.7 macrophages upon interaction with heat-inactivated *Candida*
19 *albicans* cells unravel an anti-inflammatory response. *Proteomics* **2009**, *9* (11), 2995-
20 3010.
21
22
23
24
25
26
27
28
29
30
31
32
33
34
35
36
37
38
39
40
41
42
43
44
45
46
47
48
49
50
51
52
53
54
55
56
57
58
59
60

TOC



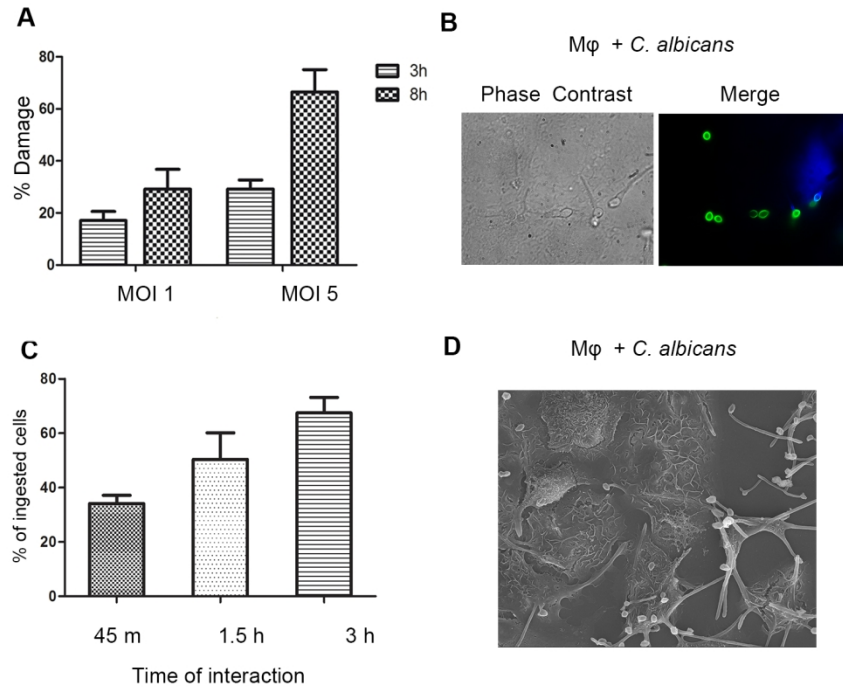


Figure 1. THP1 macrophage interaction with *C. albicans* cells. (A) Lactate dehydrogenase cytotoxicity assay to measure the damage of *Candida* cells in THP1 macrophages after 3h and 8h of interaction with *C. albicans* cells and at a MOI of 1 and 5. (B) Fluorescence microscopy images of THP1 macrophages exposed to labeled *C. albicans* strain SC5314 (Oregon green 488) in green, for 3h. Intracellular and external/adhered *C. albicans* cells were distinguished based on fluorescence after co-staining with Calcofluor white in blue, which does not enter or stain macrophages. (C) Phagocytic activity of macrophages at different times of interaction. (D) Environmental scanning electronic microscopy (ESEM) of macrophage and *C. albicans* co-culture after 3h of interaction

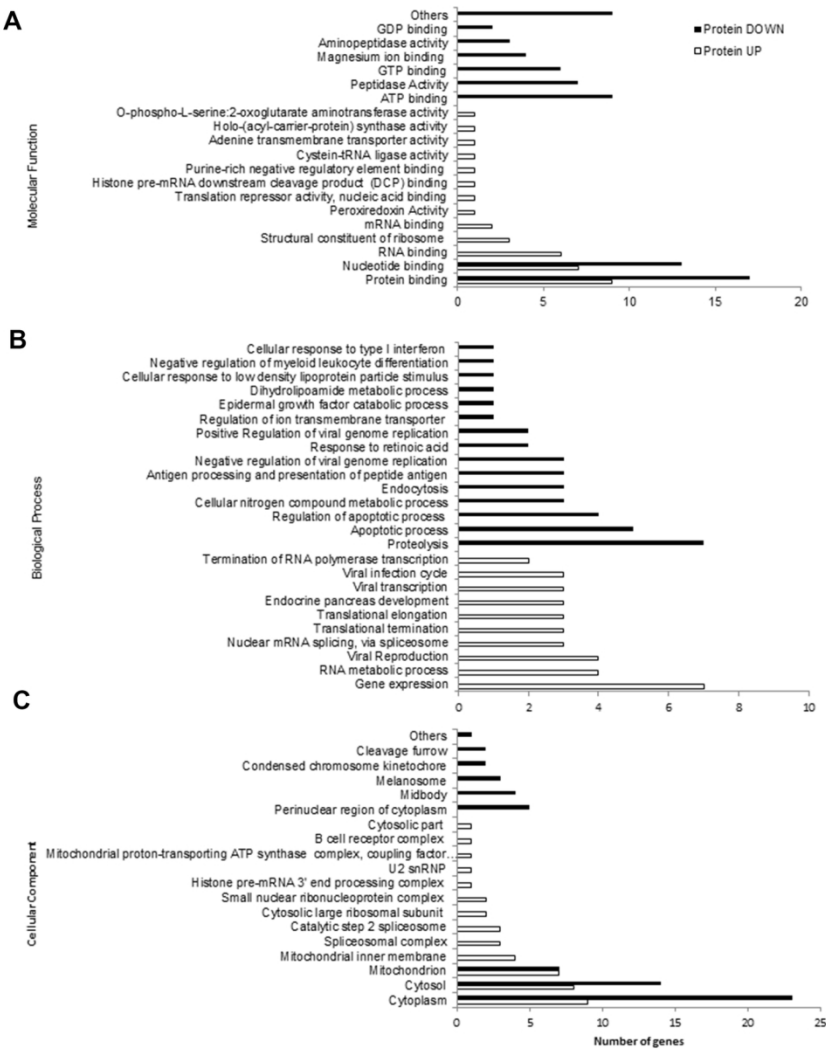


Figure 2. Gene Ontology (GO) analysis of the proteins considered differentially abundant after macrophage interaction with *C. albicans*. GO analysis of (A) molecular function, (B) biological process and (C) cellular component.

140x180mm (300 x 300 DPI)

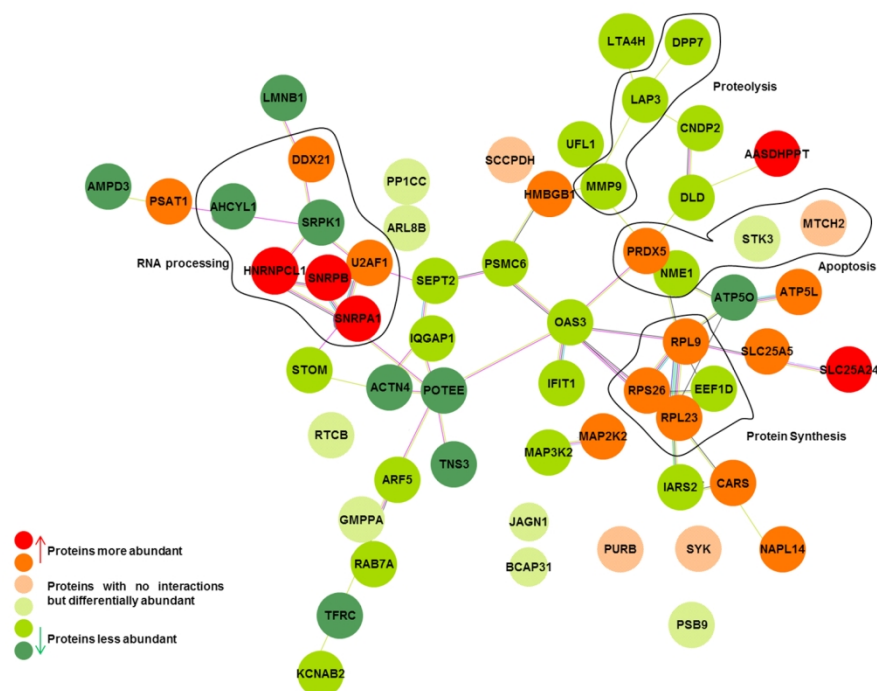


Figure 3. Predicted protein-protein interacting network using STRING (v10.0). Some biological processes (RNA splicing, protein synthesis, proteolysis, endocytic traffic and apoptosis) are highlighted in the network, signaling some of the interacting proteins that are involved in each process. The network protein-protein interaction p-value was 5.76×10^{-5} .

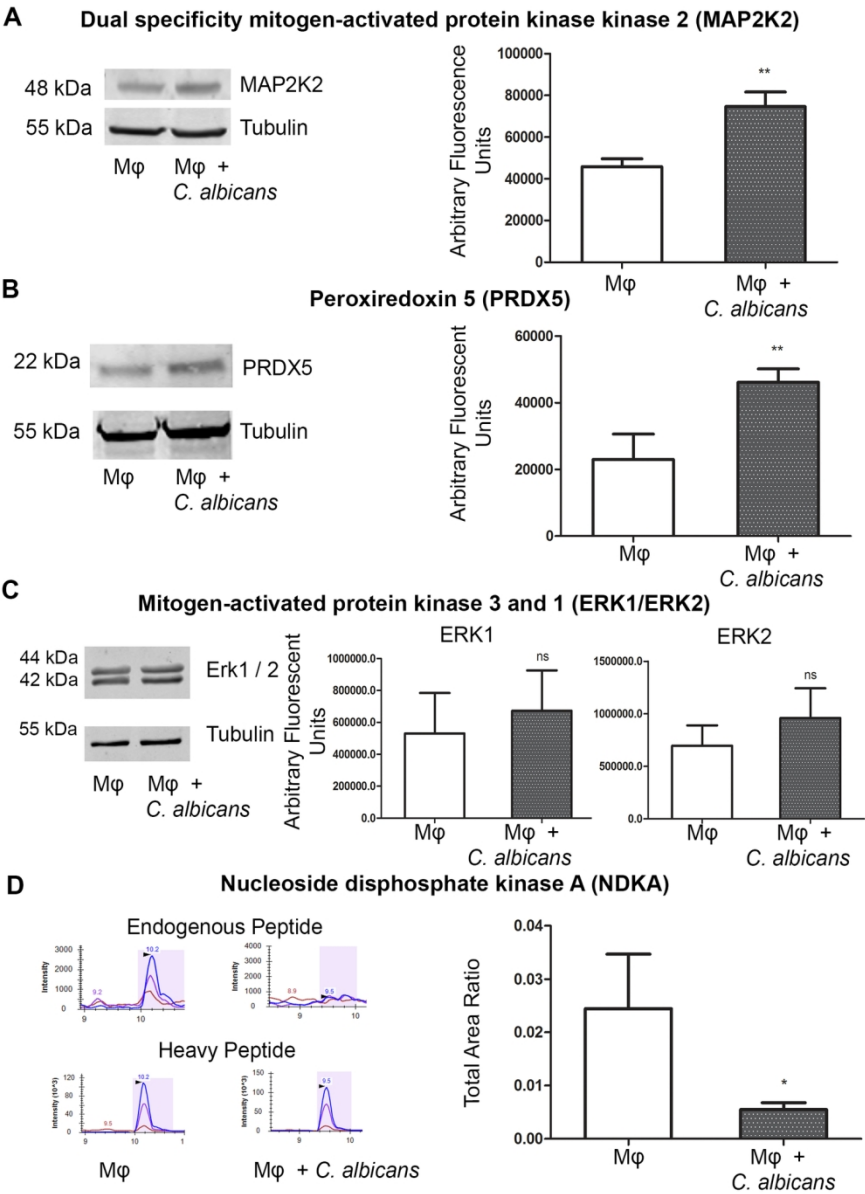


Figure 4. Proteomic results validation in both conditions: Mφ (control) and Mφ+C. albicans (MOI 1 and 3 h of incubation). Quantification of: (A) MAP2K2, (B) PRDX5 and (C) ERK1/2 by Western blotting and (D) NDKA by selected reaction monitoring.

140x180mm (300 x 300 DPI)

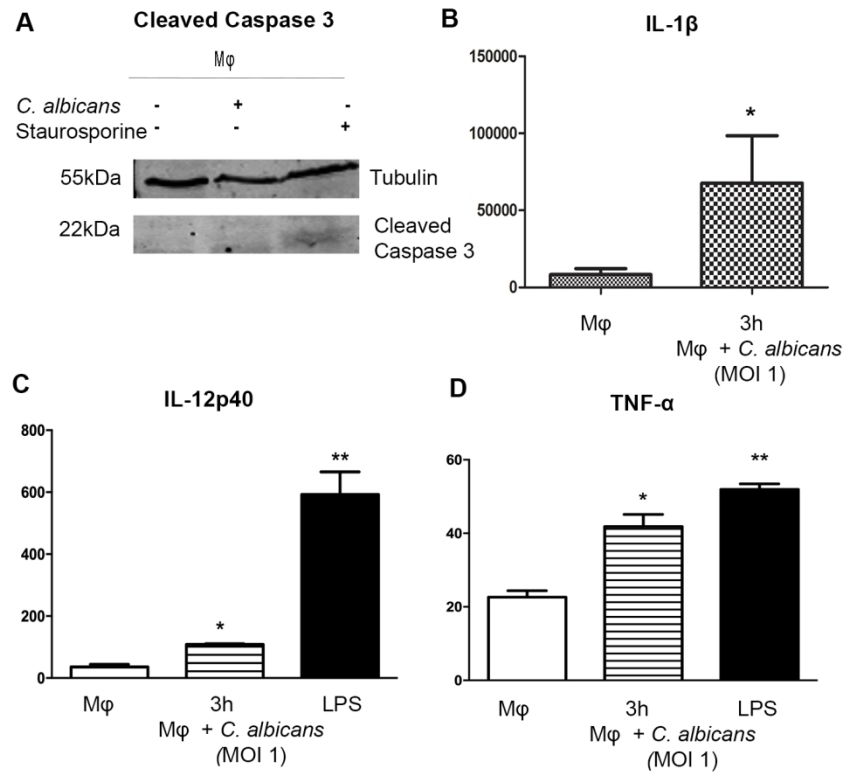


Figure 5. Caspase 3 activation and cytokine secretion measurement. Caspase activation was measured by Western blotting (A) and cytokine secretion measured using Enzyme-Linked ImmunoSorbent Assay (ELISA): (B) IL-1β, (C) IL-12p40 and (D) TNF-α secretion in Mφ (control) and Mφ+*C. albicans* and after treatment with LPS (positive control).

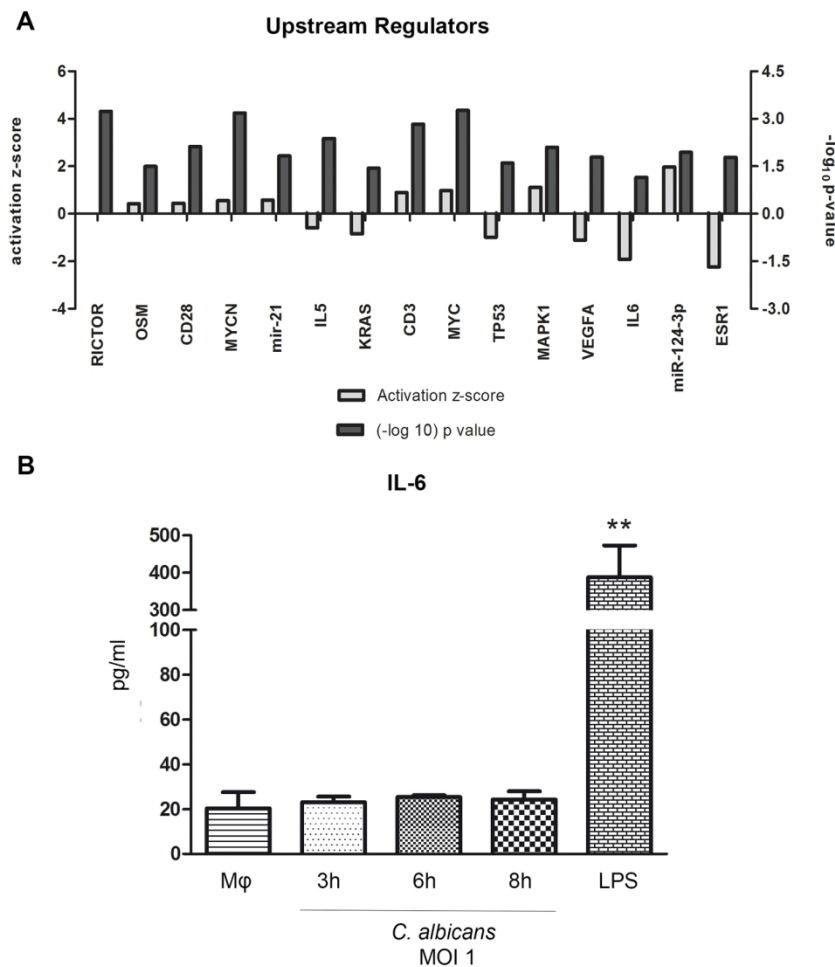


Figure 6. Upstream-regulators predicted to be implicated in the response to *C. albicans* using Ingenuity® Pathway Analysis (IPA). The upstream regulators analysis is based on prior knowledge of expected effects between transcriptional regulators and their target genes stored in the IPA. (A) Bar chart of the upstream regulators that were predicted, including the activation z-score and p-value of each upstream regulator derived from IPA. Cellular validation of some of the upstream regulators was performed (B) IL-6 secretion by ELISA.

140x180mm (300 x 300 DPI)

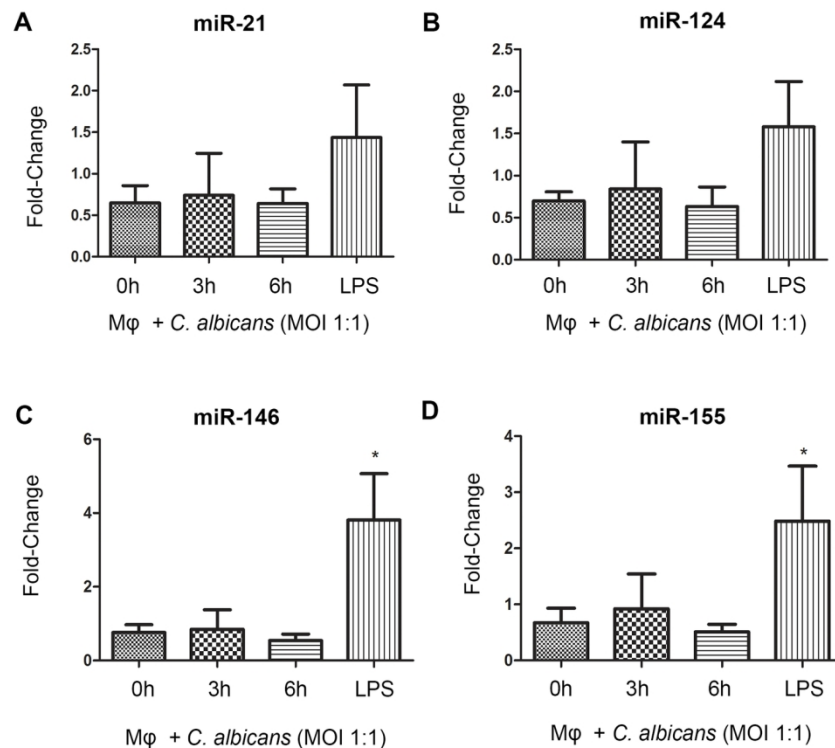


Figure 7. Expression levels of miRNAs in THP1 macrophages after interaction with *C. albicans* cells. Expression levels of (A) miR-21 and (B) mir-124 that were predicted by the IPA and (c) miR-146 and (D) miR-155 that were known to be activated after treatment with LPS and were used as controls.

140x180mm (300 x 300 DPI)

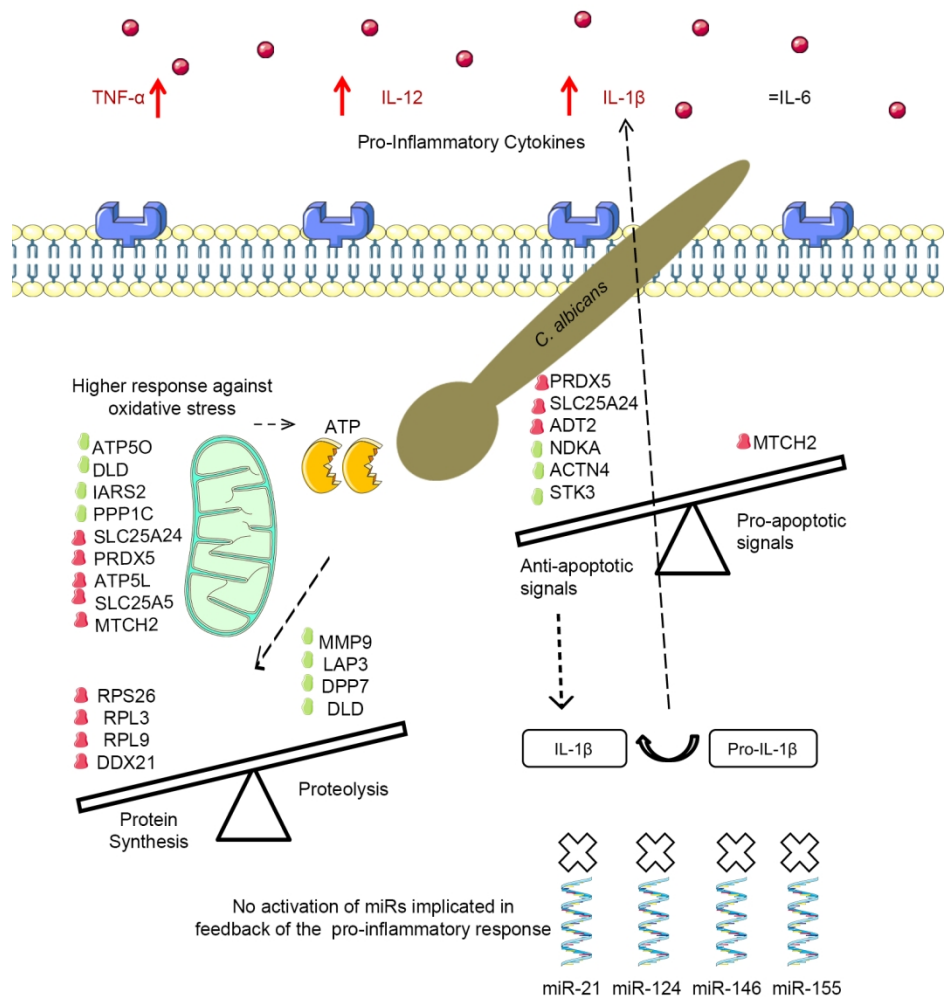


Figure 8. Schematic overview of macrophage possible remodeling after interaction with *C. albicans*. The differentially abundant proteins, together with the cytokines, are color coded with red for more abundant and green for less abundant after macrophage interaction with *C. albicans*. The cytokines and the miR that do not present differences after interaction are depicted in grey. The text describes some of the processes suggested to be remodeled after interaction.

